

Solubilities of phenol in supercritical carbon dioxide from aqueous phenol solutions
by Eric Raymond Leland

A thesis submitted in partial fulfillment of the requirements for the degree of Master of Science in Chemical Engineering
Montana State University
© Copyright by Eric Raymond Leland (1986)

Abstract:
The existing techniques for treating industrial chemical wastewater could benefit from cheaper and improved processing. Recent research has focused some attention upon supercritical fluid extraction. The purpose of this research was to experimentally measure solubilities of phenol, a common wastewater pollutant, in supercritical carbon dioxide from aqueous phenol solutions. A thermodynamic model of this system was also developed.

Extraction experiments were performed with a single pass flow apparatus. Liquid carbon dioxide was fed into the extraction cell by way of a high pressure liquids pump. The charged vapor samples were bubbled through water to isolate the product phenol. A wet chemistry, direct photometric method was used for phenol analysis. Experiments were run at 40 and 60 degrees Celsius. Aqueous phenol solutions of 10,000 parts per million, ppm, 5,000 ppm, and 2,500 ppm were studied. The pressures investigated ranged from 1,100 psi to 2,800 psi.

Measured experimental phenol mole fractions in supercritical carbon dioxide ranged from 0.000060 to 0.00080. At 40 degrees Celsius the vapor phase phenol solubility increased with increasing pressure. At 60 degrees Celsius the vapor phase phenol solubility passed through minimums over pressure at lower pressures. Larger aqueous phenol solution concentrations gave larger vapor phase phenol solubilities at both temperatures. The lower temperature of 40 degrees Celsius gave larger vapor phase phenol solubilities than at 60 degrees Celsius.

The data generated by the thermodynamic model of the aqueous phenol-supercritical carbon dioxide system passed through minimums in vapor phase phenol solubilities at both 40 and 60 degrees Celsius in the pressure range of 600 to 700 psia. The model predicted general trends at both temperatures but also showed discrepancies at both temperatures. These discrepancies might have been caused by assumptions made to solve the model.

SOLUBILITIES OF PHENOL IN SUPERCRITICAL CARBON DIOXIDE FROM AQUEOUS PHENOL SOLUTIONS

by

Eric Raymond Leland

A thesis submitted in partial fulfillment
of the requirements for the degree

of

Master of Science

in

Chemical Engineering

MONTANA STATE UNIVERSITY
Bozeman, Montana

January 1986

MAIN LIB.
N378
L538
Cop. 2

APPROVAL

of a thesis submitted by

Eric Raymond Leland

This thesis has been read by each member of the thesis committee and has been found to be satisfactory regarding content, English usage, format, citations, bibliographic style, and consistency, and is ready for submission to the College of Graduate Studies.

January 13, 1986
Date

Warren P. Scarrah
Dr. Warren Scarrah, Chairman

Approved for the Major Department

January 14, 1986
Date

John T Sears
Dr. John Sears, Department Head

Approved for the College of Graduate Studies

February 7, 1986
Date

Henry L Parsons
Dr. Henry Parsons, Graduate Dean

STATEMENT OF PERMISSION TO USE

In presenting this thesis in partial fulfillment of the requirements for a master's degree at Montana State University, I agree that the Library shall make it available to borrowers under rules of the Library. Brief quotations from this thesis are allowable without permission, provided that accurate acknowledgment of source is made.

Permission for extensive quotation from or reproduction of this thesis may be granted by my major professor, or in his/her absence, by the Director of Libraries when, in the opinion of either, the proposed use of the material is for scholarly purposes. Any copying or use of the material in this thesis for financial gain shall not be allowed without my written permission.

Signature Eric Leland

Date January 14, 1986

TABLE OF CONTENTS

	Page
APPROVAL	ii
STATEMENT OF PERMISSION TO USE	iii
TABLE OF CONTENTS	iv
LIST OF TABLES	vi
LIST OF FIGURES	vii
ABSTRACT	ix
INTRODUCTION	1
Wastewater Treatment Via Supercritical Fluids	1
Research Objectives	2
Supercritical Fluids	2
Extraction With Supercritical Fluids	3
Supercritical Fluid Applications	4
High Pressure Experimental Methods	5
Flow Methods	5
Static Methods	6
EXPERIMENTAL	7
Experimental Design	7
Experimental Apparatus	7
Experimental Procedure	10
Phenol Analysis	13
Reagents	13

TABLE OF CONTENTS--Continued

RESULTS AND DISCUSSION 14

General Observations 14
Experimental Solubilities 14
Data at 40 Degrees Celsius 15
Data at 60 Degrees Celsius 19
Thermodynamic Modeling 21
Modeling 21
Modeling Results 26
Design Considerations 31

SUMMARY 36

RECOMMENDATIONS FOR FURTHER STUDY 38

REFERENCES CITED 40

APPENDICES 42

Appendix A - Derivation of Thermodynamic Model 43
Appendix B - Computer Aided Solutions of the Thermodynamic Model of Aqueous Phenol-Supercritical Carbon Dioxide Vapor-Liquid Equilibrium 50
Appendix C - Spectrophotometric Phenol Analysis Calibration Curve of Absorbance Versus Phenol Concentration 58

LIST OF TABLES

Page

Tables

1. Mole Fraction Phenol in Supercritical Carbon Dioxide at 40 degrees Celsius 16

2. Mole Fraction Phenol in Supercritical Carbon Dioxide at 60 degrees Celsius 19

3. Aqueous Phenol-Supercritical Carbon Dioxide Model Calculated Values of Mole Fractions in the Vapor Phase, Vapor Phase Component Fugacity Coefficients, and Poynting Corrections for Phenol and Water at 60 degrees Celsius and Phenol Solution Concentration of 10,000 ppm 30

4. Experimental Mole Fractions of Phenol in Water, Mole Fractions of Phenol in Supercritical Carbon Dioxide, and Equilibrium K-values at 40 degrees Celsius 31

5. Experimental Mole Fractions of Phenol in Water, Mole Fractions of Phenol in Supercritical Carbon Dioxide, and Equilibrium K-values at 60 degrees Celsius 33

LIST OF FIGURES

Page

Figures

1. Schematic of phenol extraction apparatus 8

2. Experimental vapor phase phenol solubilities in supercritical carbon dioxide at 40 degrees Celsius . . . 17

3. Supercritical carbon dioxide density as a function of pressure at 40 and 60 degrees Celsius 18

4. Experimental vapor phase phenol solubilities in supercritical carbon dioxide at 60 degrees Celsius 20

5. Experimental vapor phase phenol solubilities in supercritical carbon dioxide at 40 and 60 degrees Celsius. . 22

6. Thermodynamic model-generated vapor phase phenol solubilities and experimental phenol solubilities in supercritical carbon dioxide at 40 degrees Celsius 27

7. Thermodynamic model-generated vapor phase phenol solubilities and experimental phenol solubilities in supercritical carbon dioxide at 60 degrees Celsius 28

8. Calculated distribution coefficients of phenol from experimental data for system pressure at 40 degrees Celsius 32

9. Calculated distribution coefficients of phenol from experimental data for system pressure at 60 degrees Celsius 34

10. Comparison of two solution methods of the aqueous phenol-supercritical carbon dioxide thermodynamic model at 40 degrees Celsius (method 1 used all three of the component fugacity equations and method 2 used two of the component fugacity equations and a vapor phase mole balance) 52

LIST OF FIGURES--Continued

Page

11. Comparison of two solution methods of the aqueous phenol-supercritical carbon dioxide thermodynamic model at 60 degrees Celsius (method 1 used all three of the component fugacity equations and method 2 used two of the component fugacity equations and a vapor phase mole balance) 53

12. Computer program to calculate the vapor-liquid equilibrium of the aqueous phenol-supercritical carbon dioxide system 54

13. Phenol analysis calibration curve of absorbance versus phenol concentration 59

ABSTRACT

The existing techniques for treating industrial chemical wastewater could benefit from cheaper and improved processing. Recent research has focused some attention upon supercritical fluid extraction. The purpose of this research was to experimentally measure solubilities of phenol, a common wastewater pollutant, in supercritical carbon dioxide from aqueous phenol solutions. A thermodynamic model of this system was also developed.

Extraction experiments were performed with a single pass flow apparatus. Liquid carbon dioxide was fed into the extraction cell by way of a high pressure liquids pump. The charged vapor samples were bubbled through water to isolate the product phenol. A wet chemistry, direct photometric method was used for phenol analysis. Experiments were run at 40 and 60 degrees Celsius. Aqueous phenol solutions of 10,000 parts per million, ppm, 5,000 ppm, and 2,500 ppm were studied. The pressures investigated ranged from 1,100 psi to 2,800 psi.

Measured experimental phenol mole fractions in supercritical carbon dioxide ranged from 0.000060 to 0.00080. At 40 degrees Celsius the vapor phase phenol solubility increased with increasing pressure. At 60 degrees Celsius the vapor phase phenol solubility passed through minimums over pressure at lower pressures. Larger aqueous phenol solution concentrations gave larger vapor phase phenol solubilities at both temperatures. The lower temperature of 40 degrees Celsius gave larger vapor phase phenol solubilities than at 60 degrees Celsius.

The data generated by the thermodynamic model of the aqueous phenol-supercritical carbon dioxide system passed through minimums in vapor phase phenol solubilities at both 40 and 60 degrees Celsius in the pressure range of 600 to 700 psia. The model predicted general trends at both temperatures but also showed discrepancies at both temperatures. These discrepancies might have been caused by assumptions made to solve the model.

INTRODUCTION

Wastewater Treatment Via Supercritical Fluids

A constant and integral part of chemical process industry is the investigation and adaptation of new or existing technologies that might improve a process's economics and/or boost its overall performance. The treatment of industrial chemical wastewater is an area that could benefit from cheaper and improved processing. Supercritical fluid extraction could be a promising method for treating wastewater.

Supercritical fluid extraction involves extraction with a fluid above its critical point (critical temperature, Tc, critical pressure, Pc). The fluid's solvent power in the critical region varies greatly with small changes in temperature and pressure. Recent applications include the decaffeination of coffee, extraction of spices, and regeneration of activated carbon. Carbon dioxide is overwhelmingly the preferred solvent in most applications. Carbon dioxide has moderate critical properties (Tc = 31 degrees Celsius, Pc = 1070 psia), is environmentally safe, readily available, and relatively inexpensive.

The prospect of using supercritical fluid extraction to treat wastewater is mentioned by Bott [1, p. 229]. However, there is little published experimental data for solubilities of common wastewater pollutants in supercritical carbon dioxide as a function of pressure and temperature. Also most of the solubilities are for pure materials. In order to further assess the potential of supercritical carbon dioxide in treating wastewater there is a need to investigate aqueous waste solutions. Van Leer and Paulaitis have reported the solubilities

of a common wastewater pollutant, phenol, in supercritical carbon dioxide as a function of pressure [2, pp. 257-259]. They demonstrated that supercritical carbon dioxide is an effective solvent for phenol. Therefore, an investigation into the solubilities of aqueous phenol solutions in supercritical carbon dioxide appears worthwhile.

Research Objectives

The primary objective of this research was to measure experimental vapor liquid equilibrium data for the aqueous phenol-supercritical carbon dioxide system. Experimental apparatus and procedures were developed to create a reproducible system. A thermodynamic model of the above mentioned system was developed to predict vapor and liquid phase compositions at equilibrium.

Supercritical Fluids

Pure fluids are generally thought of as liquids and gases. This is true for most fluids up to a specific point called the critical point, here the two phases become indistinguishable. The critical point has the coordinates of critical temperature and critical pressure. Above the critical temperature it is not possible to liquefy the fluid at any pressure. The critical pressure is the pressure required to liquefy the fluid at its critical temperature. A discussion of the critical region of pure fluids and a physical description of a fluid at its critical point is provided by Smith and Van Ness [3, pp. 57-60].

Extraction With Supercritical Fluids

The inherent physical properties of supercritical fluids are very attractive from the standpoint of a separation technique. The following description of these properties is given by Bott [1, p. 229]. In its supercritical state the dense fluid is very mobile. The fluid has a density of up to one-third or more compared to the liquid state, while its viscosity can be as low as one-fifth or less depending on pressure and temperature. This results in fluid solubilities approaching those of the liquid phase yet the fluid can penetrate faster and deeper into a solid matrix of natural substances or could progress faster through a densely packed fixed bed or column.

Extraction via supercritical fluids is characterized by the following features which are provided by Wilke [4, p. 701]: (1) relatively involatile materials can be dissolved by supercritical fluids, sometimes even selectively, (2) phenomena of distillation and extraction are simultaneously involved, i.e. enhancement of vapor pressure and phase separation both play a role, (3) the properties of the supercritical fluid such as density can be varied within wide limits by means of pressure and temperature, and (4) separation of the dissolved substances can be accomplished either by a reduction of pressure (at constant temperature) or by raising temperature (at constant pressure). Two additional features are given by Bott [1, p. 229]: (1) the lower operating temperatures involved allow for the successful extraction of heat sensitive compounds, and (2) the use of supercritical carbon dioxide leaves no harmful residues.

Supercritical fluid extraction is a relatively high pressure process. High pressure processes are recognized as high cost operations due to expensive equipment and energy demands to maintain plant pressure. These costs may be prohibitive to supercritical fluid extraction unless there is some type of energy recovery and/or a process enjoys key advantages from using supercritical fluid extraction. There is very little published information on the costs of supercritical fluid extraction. An article by Peter and Brunner discussed data on the costs of separation of non-volatile substances [5, pp. 746-750].

Supercritical Fluid Applications

Chemical process industries have begun to exploit the uses of supercritical fluids. An article by Kohn and Savage reviews promising applications of supercritical fluids, but it is without references [6, pp. 41-43].

Supercritical carbon dioxide has demonstrated an affinity towards some natural product constituents such as caffeine in coffee and extracts of spices. An article by Zosel gives a description of the decaffeination of coffee via supercritical carbon dioxide [7, pp. 707-709]. Hubert and Vitzhum provide an introduction to the methods of supercritical carbon dioxide extraction of hops, spices, and tobacco in their article [8, pp. 710-715].

Supercritical carbon dioxide is also being used to regenerate activated carbon [9].

The uses of supercritical fluids are finding applications in the fuels industry. Kerr-McGee has commercialized a process that extracts asphaltenes and residues from distillation residue in oil refineries using supercritical aliphatic hydrocarbons [6, pp. 41-42]. Britain's National Coal Board Research Establishment is using supercritical toluene to extract light hydrocarbons from coal leaving behind a charred residue [6, pp. 42-43].

High Pressure Experimental Methods

There are two general approaches to measuring high pressure vapor-liquid equilibrium. These are flow systems and static systems. An article by Young describes these systems in general and also presents specific experimental systems that have been used [10, pp. 83-104].

Flow Methods

There are two types of flow systems, the single pass system, and the vapor recirculation system. In the single pass system a sample of pure gas at a specified pressure is passed through a liquid at a specified temperature. In a given length of time the liquid and vapor are essentially in equilibrium, which in a well designed system is less than fifteen minutes [10, p. 83]. When equilibrium is reached samples of vapor and liquid are withdrawn for analysis.

The vapor recirculating method starts with liquid and vapor in a vessel at a specified temperature and pressure. Vapor is withdrawn and recirculated through the liquid, this vapor-liquid contact allows for a rapid approach to equilibrium. When equilibrium is reached samples of vapor and liquid are withdrawn for analysis.

The single pass method suffers from two major disadvantages with respect to the vapor recirculation method. First, it is difficult to establish whether equilibrium has been reached in one pass or not. The second disadvantage involves the pressurizing of the vessel containing liquid. All of the vapor used to pressurize the vessel contacts the liquid below the specified pressure. To insure that the vapor sample withdrawn is representative of the operating pressure, the vessel must either have enough vapor passed through it to "clear" out the initial vapor or the vessel's contents must be mixed at operating conditions.

Static Methods

There are several types of equipment systems for measuring static high pressure equilibrium. A typical method consists of placing a two-phase mixture in a sealed vessel at a specified temperature and pressure. Then the vessel's contents are mixed and when equilibrium is reached vapor and liquid samples are withdrawn for analysis. There is one major disadvantage to static methods. The pressure is usually not held constant while samples are being withdrawn, which can lead to considerable error.

EXPERIMENTAL

Experimental Design

The experimental work was performed in three stages. The first stage was the development of a working and reliable extraction apparatus. Next a series of experiments were performed to develop a practical experimental procedure with reproducible results. These experiments also gave the investigator a feel for the apparatus. The last stage was the gathering of useful data. The first set of data was at 40 degrees Celsius. Here, phenol solution concentrations of 10,000 ppm, 5,000 ppm, and 2,500 ppm were investigated over the pressure range of 1,100 psig to 2,800 psig. The second set of data was at 60 degrees Celsius. Phenol solution concentrations of 10,000 ppm and 2,500 ppm were investigated over the same pressure range as at 40 degrees Celsius.

Experimental Apparatus

A schematic of the experimental apparatus appears in Figure 1. The apparatus used was a single pass flow system. An inverted carbon dioxide gas cylinder was used to feed liquid carbon dioxide to the liquids pump. A Milroy Model HBD-1-30R high-pressure liquid pump was used to pressurize the extraction cell and to deliver carbon dioxide to the extraction cell at constant pressures. The pump was charged with ambient temperature carbon dioxide by a carbon dioxide gas cylinder which was inverted to deliver liquid solvent. The pump's liquid end was always packed in ice to keep the carbon dioxide liquid in the pumping chamber and thus insuring consistent flow by preventing a vapor

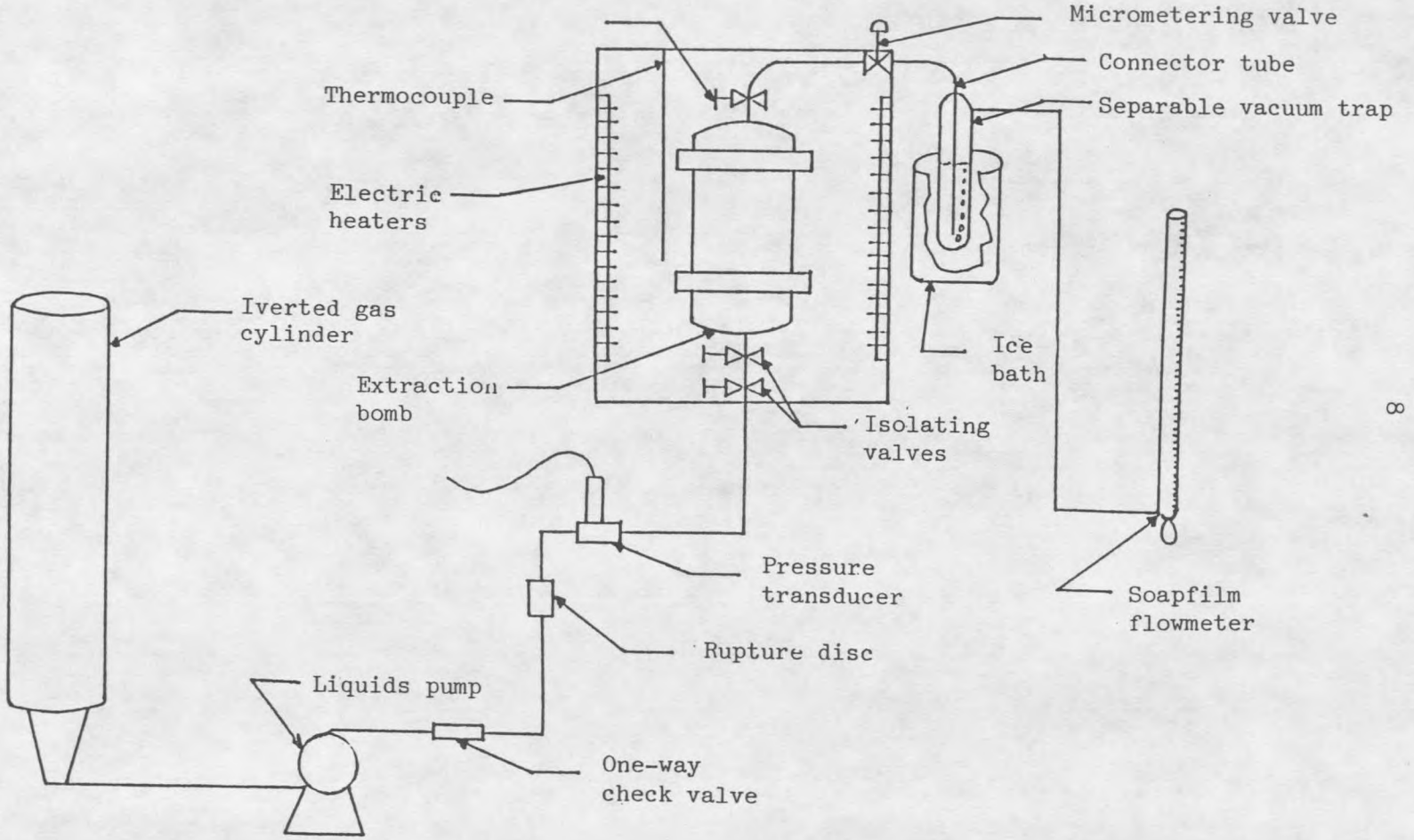


Figure 1. Schematic of phenol extraction apparatus

lock. Pumping liquid carbon dioxide yielded consistent flow and stable system pressures. The pump was protected by a rupture disc and a one-way check valve located beyond the pump and before the extraction cell.

The extraction cell was a one-liter monel bomb rated at 3,500 psi suspended in an electrically heated oven. Eighty percent of the bomb's volume was packed with 0.64 centimeter ceramic Berl saddles. This left a two hundred millileter empty space and roughly a height of six centimeters for vapor-liquid disengagement. Oven temperature was controlled by electrical heaters controlled by a Powerstat type 3PN1168 variable auto transformer. There was a network of valves around the bomb which allowed for the isolation and removal of the bomb while under pressure.

A Whitey Model number SS-22RS4 micrometering valve was used to control pressure and collect samples for analysis. This valve flashed the saturated vapor to atmospheric pressure. Then the flashed vapor bubbled through a separable vacuum trap containing seventy-five milliliters of deionized water that was held at 0 degrees Celsius by means of an ice bath. Then the "clean" vapor was routed through a one hundred milliliter soap film flowmeter and then to the atmosphere. Initially an attempt was made to collect phenol samples in a dry trap held at 0 degrees Celsius by an ice bath. This failed to produce any detectable traces of phenol in the trap. Therefore, the alternative method of using deionized water in the trap was employed, and was satisfactory. The failure of the first attempt might have been caused by the small size of the condensed phenol particles which may have been carried through the trap by the effluent vapor flow.

System pressures were monitored by an Autoclave Engineers Model DPS0081 pressure sensor and an Autoclave Engineers Model DPT418 pressure transducer. The pressure transducer was located before the extraction cell by roughly 1.5 meters of tubing. A calculation of pressure drop over this distance due to frictional flow was made and was negligible. Oven temperature was monitored by a Cole Palmer Model 8530 thermometer and a thermocouple in the oven.

Phenol analysis used the following equipment; an Orion 901 ionalyzer used as a pH meter; a Bausch and Lomb Spectronic 20 spectophotometer; a magnetic stirrer; and a mass balance.

Experimental Procedure

Preparation for an experimental run began the evening before. The bomb was charged with fresh solution if necessary. Phenol solutions were prepared from reagent grade phenol and deionized water. The bomb needed to be recharged if the next run required a different phenol solution concentration. Charging the bomb with fresh solution involved gravimetrically filling the bomb with roughly six hundred milliliters of the desired solution, which filled the bomb to the level of its packing. Next the bomb was clamped into the oven which had been preheated to the run temperature. Then the bomb was connected to the system's tubing and pressurized with saturated carbon dioxide at room temperature, roughly 900 psi. The bomb was then sealed from the system and heated up to the run temperature overnight.

The experimental run began the next morning. First the pump was used to bring the system up to the operating pressure and then

maintained at this pressure for 15 minutes. Next the bomb was isolated from the system and removed from the oven for mixing. This mixing insured intimate vapor-liquid contact at operating pressure. When the bomb reached operating pressure, virtually all of the carbon dioxide in the bomb, roughly 200 milliliters, had been bubbled through the liquid at sub-operating pressure. This included the pressurizing of the bomb with saturated carbon dioxide at room temperature and the pumped carbon dioxide that brought the bomb up to operating pressure. All of this carbon dioxide remained in the bomb since the outlet of the bomb was closed to flow. Therefore, the vapor and liquid in the bomb needed to be re-contacted at operating conditions. Upon reaching operating pressure and after a 15 minute wait, the bomb was isolated and removed from the oven and shaken vigorously for roughly one minute. Then the bomb was clamped back into the oven and opened up to the system. The bomb's drop in pressure during removal from the oven ranged from less than 10 psi up to 50 psi. The larger pressure drops were associated with higher operating pressures and all pressure drops were corrected within 5 minutes. These pressure drops were probably due to the slight cooling of the bomb upon oven removal. When the bomb pressure had been restored it was maintained for one hour.

After the one hour period a sample of vapor was ready to be withdrawn. The micrometering valve was opened to deliver a desirable flow, which ranged from 50 milliliters per minute to 200 milliliters per minute. The phenol in the vapor sample was condensed out of the vapor in the separable vacuum trap, and was also deposited in the micrometering valve and on the connecting tube. The vapor flowrate was

measured with the soap film flowmeter and a stop watch. The amount of carbon dioxide from each run ranged from around 4,500 milliliters to 6,000 milliliters at ambient conditions. Ambient pressure was recorded along with effluent vapor temperature. During the run and the hour period before sample collection pressure was always held to $\pm$ 10 psi and usually held to $\pm$ 5 psi. Also during this time oven temperature was held to $\pm$ 1 degree Celsius. During the experimental run the phenol solution was depleted somewhat. The amount of solution depletion was small due to the relatively large amount of liquid solution and the small solubilities of phenol in the vapor phase. The phenol solution concentration was always within 95% of the stated concentration.

When the sample had been taken, the micrometering valve was isolated from the system. Then the valve, connecting tube, and separable vacuum trap were removed as a unit, and then taken to the lab for phenol recovery. Only these components were used in phenol recovery because they were the only components that were exposed to the phenol in the vapor sample collected during the run. Here all the components were thoroughly washed with 175 milliliters of deionized water and all of the washings plus the contents of the trap were placed in a tightly-sealed, labled, and tared sample bottle. Then the sample bottle was weighed and stored for later phenol analysis. Also after each run, the 0.16 centimeter O.D. stainless steel tubing that ran from the bomb to the micrometering valve was washed out with deionized water. This insured that the next run would not be influenced by phenol that might have been left in the tubing from the previous run.

Phenol Analysis

The phenol analysis was a direct photometric method. The actual wet chemistry is presented in Standard Methods For the Examination of Water and Wastewater [11, pp. 510-513]. A series of phenol standards was prepared and analyzed by the above procedure. From this a calibration curve was constructed, which plotted absorbance versus phenol concentration (appendix C). The absorbance readings of unknowns were compared against the calibration curve and phenol concentrations were read directly off the curve. Phenol analyses were performed on three known prepared solutions and repeated on a couple of experimental samples in order to evaluate the accuracy of the phenol analysis. All analyses were within 5% error.

The calculation of phenol mole fraction in the vapor samples was accomplished by individually calculating the amounts of carbon dioxide and phenol. The amount of phenol was calculated from knowing the phenol concentration of the collected water sample and its mass. The amount of carbon dioxide was calculated from the ideal gas law. Ambient temperature and pressure were known along with sample volume.

Reagents

All chemicals used were reagent grade except carbon dioxide. The carbon dioxide was welding grade and was 99.9% pure. The water used was deionized.

RESULTS AND DISCUSSION

General Observations

Phenol solubilities were measured at a constant temperature and at a constant phenol solution concentration over a range of pressures. As previously mentioned the depletion of phenol during a run changed the aqueous phenol concentration less than 5%. Also as mentioned before phenol analysis by the direct photometric method produced results with less than 5% error.

The critical properties of the supercritical phase mixture (Tc, Pc) were assumed to be identical to those of pure carbon dioxide (Tc = 31 degrees Celsius, Pc = 1070 psia) and unaffected by the presence of phenol and water since they were in such small concentrations.

Experimental Solubilities

The primary objective of this research was to measure experimental solubility data for phenol in supercritical carbon dioxide from aqueous phenol solutions. The parameters studied during these vapor-liquid equilibrium runs were temperature, pressure, and phenol solution concentration. Solution concentrations were reported in parts per million, ppm, which was a weight ratio (e.g. 10,000 ppm was 1 weight % phenol).

The reported phenol solubilities were for temperatures of 40 degrees Celsius and 60 degrees Celsius, and were mole fraction phenol in the vapor phase. Each experimental run was duplicated and the difference between replicates averaged 17%.

Data at 40 Degrees Celsius

The phenol solubilities for 40 degrees Celsius are listed in Table 1. This data includes the values for each experimental replicate and the average. For this temperature the following three phenol solution concentrations were investigated: 10,000 ppm; 5,000 ppm; and 2,500 ppm. The pressure range investigated for each of these solution concentrations was 1,100 psig to 2,800 psig. The average values for each duplicated experiment are plotted in Figure 2.

The effect of pressure upon vapor phase phenol solubility was consistent among the three phenol solution concentrations. The vapor phase phenol solubility increased significantly in the pressure range of 1,100 psig to 2,000 psig. Beyond 2,000 psig the vapor phase phenol solubility leveled off indicating a much weaker function of pressure. Figure 2 also shows that increased phenol solution concentration gave larger vapor phase phenol solubilities.

The effect of pressure on vapor phase phenol solubility was similar to its effect on supercritical carbon dioxide density (Figure 3).

The density increased rapidly with increased pressure in the same pressure range as did vapor phase phenol solubility. Also the density started tapering off at roughly the same pressure as did the vapor phase phenol solubility. It was apparent that increased density in the vapor phase resulted in increased solute solubility in the vapor phase.

Table 1. Mole Fraction Phenol in Supercritical Carbon Dioxide at 40 degrees Celsius

10,000 ppm				5,000 ppm				2,500 ppm			
Press	Mole Fraction Phenol			Press	Mole Fraction Phenol			Press	Mole Fraction Phenol		
(Psig)	Exp. 1	Exp. 2	Ave.	(Psig)	Exp. 1	Exp. 2	Ave.	(Psig)	Exp. 1	Exp. 2	Ave.
1100	0.000095	0.00013	0.00011	1100	0.00012	0.000086	0.00010	1100	0.000069	0.000071	0.000070
1200	0.00026	0.00022	0.00024	1200	0.00020	0.00019	0.00020	1200	0.000048	0.000068	0.000058
1400	0.00034	0.00032	0.00033	1400	0.00016	0.00022	0.00019	1400	0.000096	0.00011	0.00010
1800	0.00051	0.00087	0.00069	1700	0.00025	0.00034	0.00030	1700	0.00013	0.00015	0.00014
2600	0.00080	0.00083	0.00082	2000	0.00057	0.00039	0.00048	2000	0.00018	0.00019	0.00019
				2800	0.00060	0.00041	0.00051	2800	0.00019	0.00027	0.00023

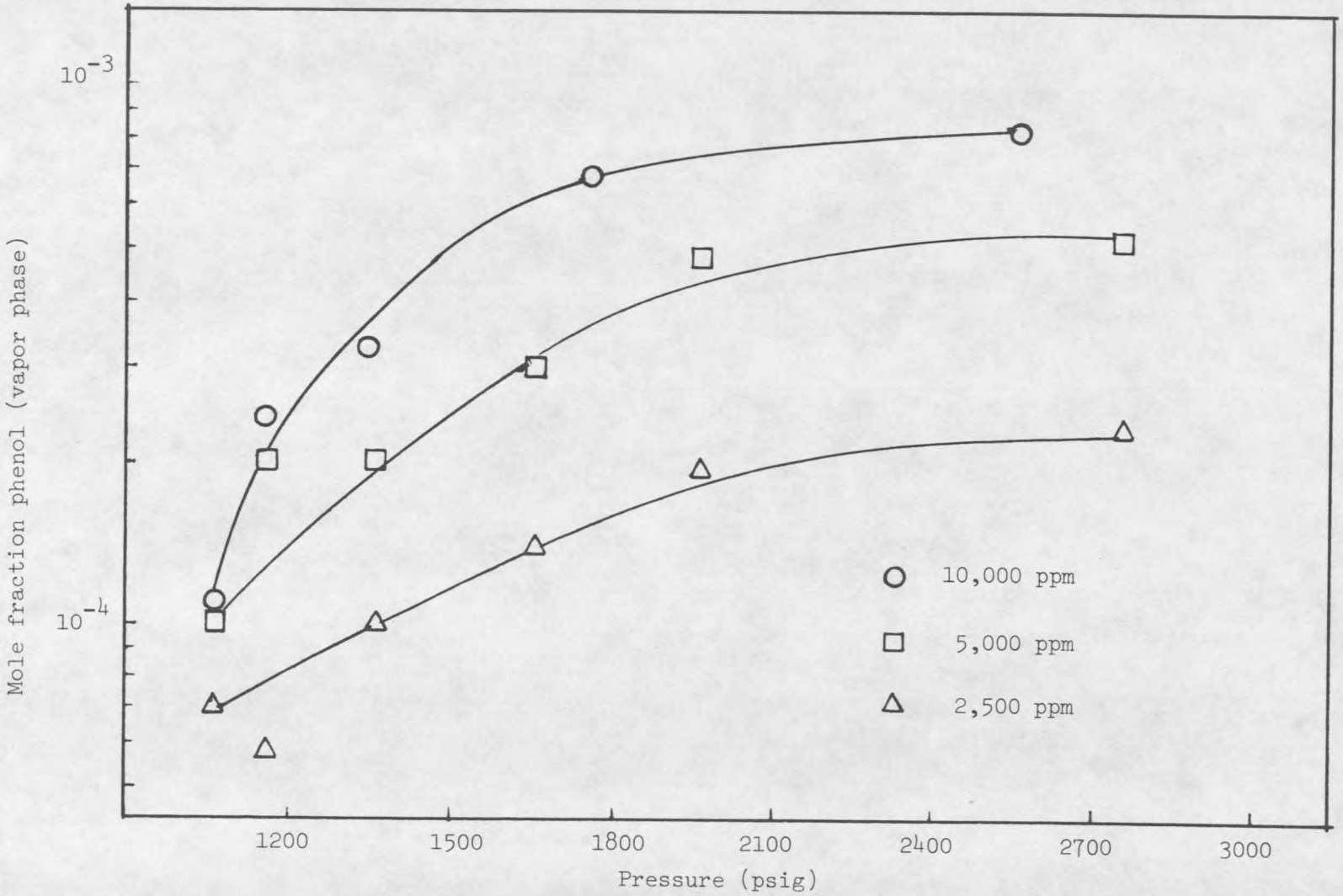


Figure 2. Experimental vapor phase phenol solubilities in supercritical carbon dioxide at 40 degrees Celsius

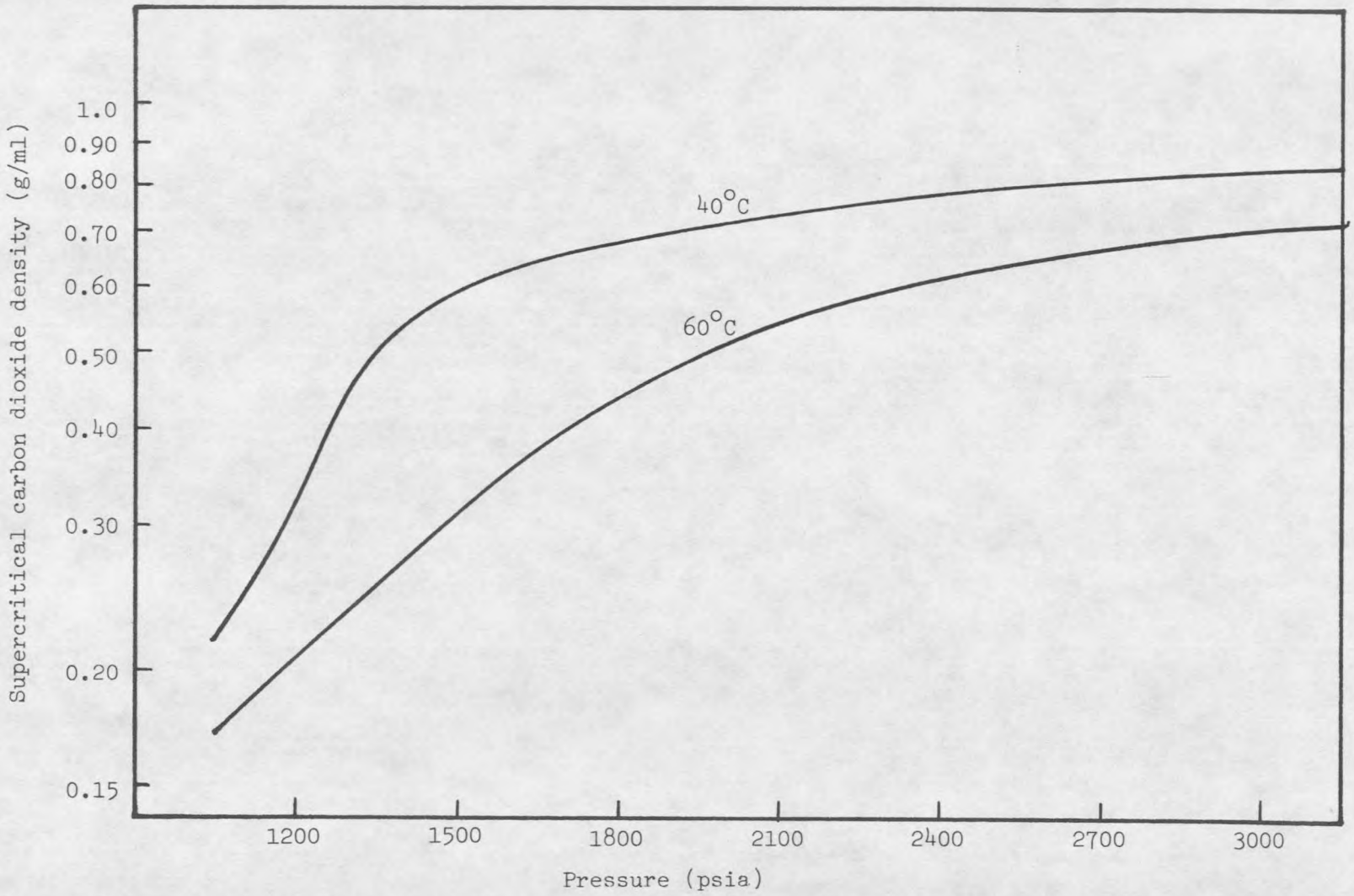


Figure 3. Supercritical carbon dioxide density as a function of pressure at 40 and 60 degrees Celsius

Data at 60 Degrees Celsius

The vapor phase phenol solubility data at 60 degrees Celsius appears in Table 2. The phenol solution concentrations investigated were 10,000 ppm and 2,500 ppm over the pressure range of 1,100 psig to 2,800 psig. This data is plotted in Figure 4.

At 60 degrees Celsius the behavior of vapor phase phenol solubility as a function of pressure was distinctly different than the behavior observed at 40 degrees Celsius. Both the Figure 4 curves at 60 degrees Celsius showed a minimum in vapor phase phenol solubility at the lower pressures, which was unexpected. This behavior was clearly shown for the data collected from the 2,500 ppm aqueous phenol solution which had nearly twice as many points as the 10,000 ppm solution.

Table 2. Mole Fraction Phenol in Supercritical Carbon Dioxide at 60 Degrees Celsius.

10,000 ppm				2,500 ppm			
Press	Mole Fraction Phenol			Press	Mole Fraction Phenol		
(Psig)	Exp. 1	Exp. 2	Ave.	(Psig)	Exp. 1	Exp. 2	Ave.
1100	0.00013	0.00011	0.00012	1100	0.000097	0.00010	0.000099
1200	0.000094	0.00010	0.000097	1200	0.000088	0.000072	0.000080
1400	0.000072	0.000084	0.000078	1300	0.000083	0.000073	0.000078
1600	0.00010	0.00014	0.00012	1400	0.000062	0.000060	0.000061
2000	0.00018	0.00015	0.00017	1550	0.000055	0.000067	0.000061
2700	0.00030	0.00037	0.00034	1650	0.000058	0.000065	0.000062
				1800	0.000068	0.000081	0.000075
				1950	0.000068	0.000082	0.000075
				2100	0.000076	0.000086	0.000081
				2300	0.000094	0.00012	0.00011
				2800	0.00015	0.00012	0.00014

The reasons why vapor phase phenol solubility experienced these depressions were not understood and led to the modeling studies described in the next section. The density versus pressure behavior

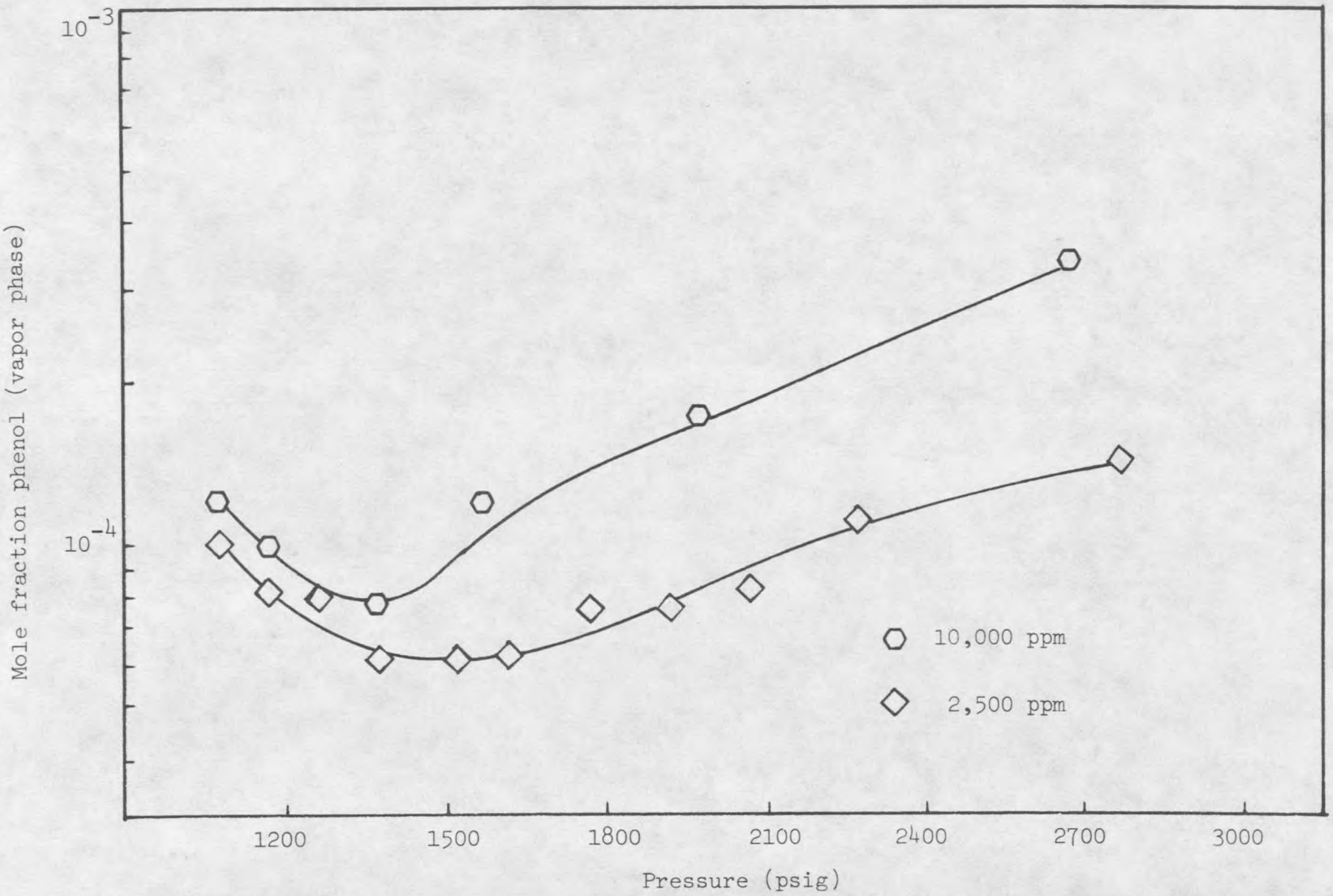


Figure 4. Experimental vapor phase phenol solubilities in supercritical carbon dioxide at 60 degrees Celsius

for carbon dioxide at 60 degrees Celsius was similar to the curve at 40 degrees Celsius (Figure 3). Obviously a different type of phenomena was taking place at 60 degrees Celsius than was at 40 degrees Celsius.

The effects of phenol solution concentration on vapor phase phenol solubility were similar to the effects at 40 degrees Celsius. Larger phenol solution concentrations gave larger vapor phase phenol solubilities.

All of the data at 40 and 60 degrees Celsius are plotted in Figure 5. The major effects of temperature on vapor phase phenol solubilities were the minimum solubilities observed at 60 degrees Celsius. The other temperature effect involved the relative magnitudes of vapor phase phenol solubilities; the higher temperature of 60 degrees Celsius gave lower values of vapor phase phenol solubility than did 40 degrees Celsius. This was probably due to the decreased carbon dioxide density at higher temperatures (Figure 3).

Thermodynamic Modeling

Modeling

A model of the aqueous phenol-supercritical carbon dioxide system was developed to calculate the system's vapor-liquid equilibrium. The model consisted of three solution component fugacity equations. Each equation involved setting the component fugacity in the supercritical state equal to the corresponding component fugacity in the liquid

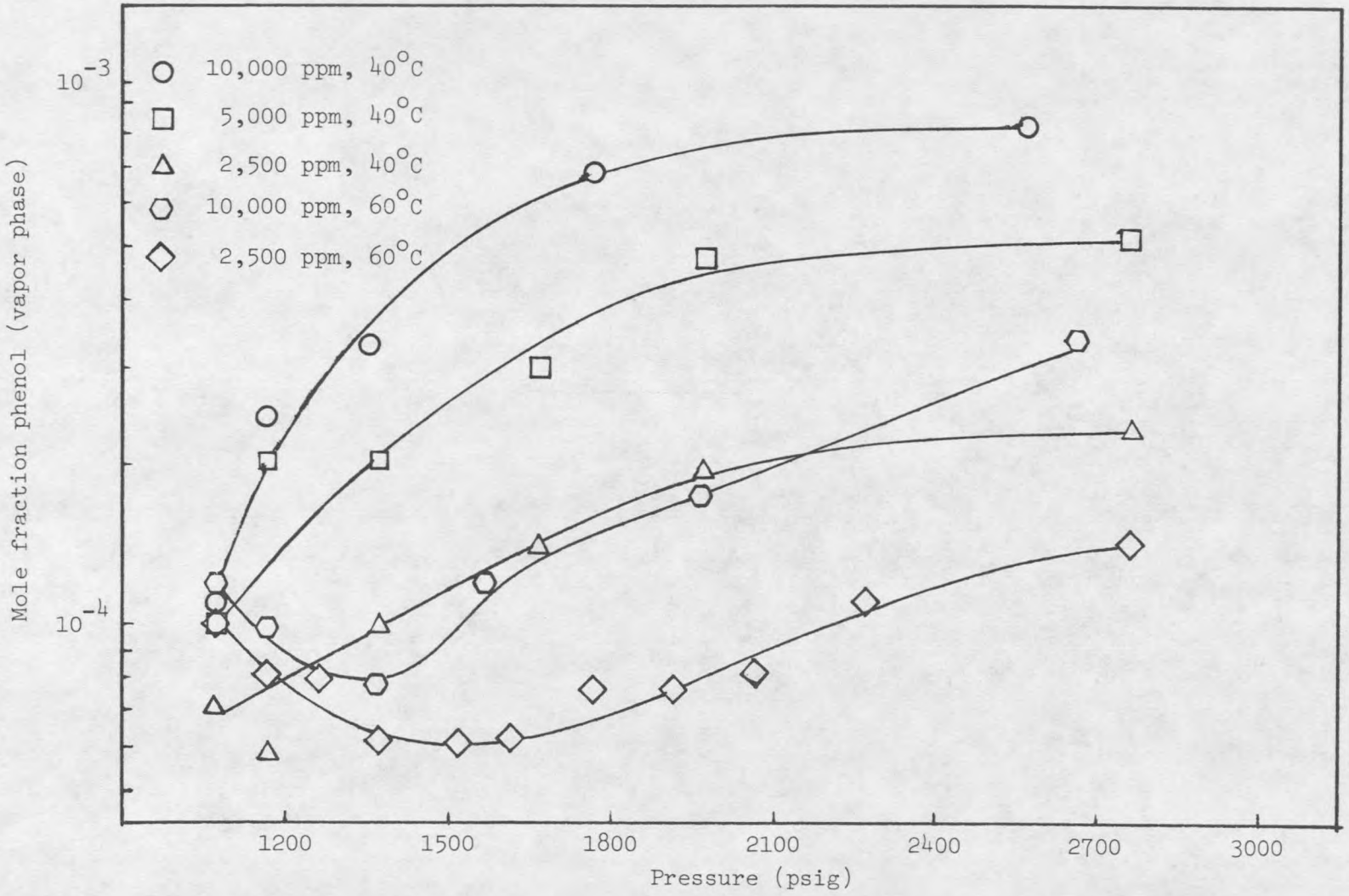


Figure 5. Experimental vapor phase phenol solubilities in supercritical carbon dioxide at 40 and 60 degrees Celsius

phase, which is a thermodynamic criterion for phase equilibrium. The three equations are listed below.

1) $y_1 \hat{\phi}_1 P = x_1 \gamma_1 f_1^0$

2) $y_2 \hat{\phi}_2 P = x_2 \gamma_2 f_2^0$

3) $y_3 \hat{\phi}_3 P = x_3 H_3$

Where:

y_i = Mole fraction of "i" in vapor phase

$\hat{\phi}_i$ = Vapor phase component fugacity coefficient of "i"

P = System pressure

x_i = Mole fraction of "i" in liquid phase

γ_i = Activity coefficient of "i" in liquid phase

f_i^0 = Standard state fugacity of "i"

H_i = Henry's law coefficient of "i"

Phenol is denoted by the subscript 1, water is denoted by 2, and supercritical carbon dioxide is denoted by 3. The unknowns in these equations were vapor phase mole fractions and vapor phase component fugacity coefficients. The component fugacity coefficients were calculated using the Peng-Robinson equation of state (appendix A) and were functions of vapor phase mole fractions, temperature, and pressure [12, p. 205]. Three-component data for liquid phase activity coefficients and for carbon dioxide solubilities in the liquid phase were not available. However, two-component Wilson parameters for phenol and water at low pressures were available to calculate liquid phase activity coefficients for phenol and water from the Wilson equation [13, pp. 754-757]. These calculated activity coefficients ignored the effects of dissolved carbon dioxide in the liquid phase and

the effects of the system's high pressures. Henry's law coefficients at elevated pressures were available for carbon dioxide and water to calculate carbon dioxide solubilities in the liquid phase [14, p. 3-96]. These calculated carbon dioxide solubilities ignored the effects of phenol in the liquid phase.

It was felt this lack of data for the three component liquid solution would not prevent the prediction of trends for the phenol solubilities in the supercritical phase. It is unlikely the small amount of dissolved carbon dioxide (less than 4 mole %) would affect the water-phenol interactions; the phenol has little tendency to interact with the carbon dioxide and is also present in very small concentrations (less than 0.2 mole %). Although the phenol-water activity coefficient data was at small pressures (2-14.7 psia) relative to system pressures (up to 2800 psig) it should be only weakly affected since the activity coefficient is a weak function of pressure. A detailed outline of equation derivation and referenced data appears in appendix A.

The component fugacity equations were solved using a trial and error computation that satisfied all three equations.

Initially an attempt was made to solve the thermodynamic model by using all three of the component fugacity equations. The solutions generated by this method gave vapor phase compositions whose sums were greater than one and this was corrected by normalizing the vapor phase composition. Unfortunately because these sums were larger than one,

the method of solution using all three of the component fugacity equations became indeterminate at elevated pressures as described below.

There was a term in the Peng-Robinson equation of state that took the natural logarithm of a difference involving vapor phase compressibility and vapor phase composition. For increased pressure this difference became smaller because the value of the vapor phase carbon dioxide mole fraction became greater than one and grew with increased pressure. Finally a pressure was reached where the difference became zero or negative and the equation of state became indeterminate. This occurred in the middle of the pressure range of the experimental data at both 40 and 60 degrees Celsius and thus, it was not satisfactory for comparison with the experimental data. Therefore this method of solution involving all three of the component fugacity equations was abandoned and an alternative method was developed.

The second method used the phenol and water component fugacity equations and a vapor phase mole balance that set the sum of the component vapor phase mole fractions equal to one. The supercritical carbon dioxide component fugacity equation was replaced by the mole balance because it was causing the indeterminate solutions.

This alternative method calculated vapor phase phenol solubilities for the entire pressure range (0-2800 psia). A comparison of the two methods showed they were similar over pressure where they both could be used; therefore the second method was selected for the modeling

studies. Appendix B shows this comparison of the two methods and also contains the computer program used to calculate the second method.

Modeling Results

The experimental vapor phase phenol solubilities at 40 degrees Celsius and phenol solution concentrations of 10,000 ppm and 2,500 ppm are plotted against their corresponding data generated by the thermodynamic model in Figure 6. In Figure 7 the same experimental and model-generated data is plotted for 60 degrees Celsius.

All of the model-generated data at both 40 degrees Celsius and 60 degrees Celsius showed a minimum in vapor phase phenol solubility at lower pressures. At 40 degrees Celsius the minimums in vapor phase phenol solubilities occurred around 600 psia while at 60 degrees Celsius the minimums occurred around 700 psia.

The mole fraction of phenol in the supercritical phase was the product of four terms: $y_i = \frac{P_i^{SAT}}{P} \times \frac{1}{\hat{\phi}_i} \times x_i \gamma_i \times \exp\left[\frac{V_i}{RT}(P - P_i^{SAT})\right]$

The first term, called the ideal solubility, showed that the vapor phase phenol mole fraction was inversely proportional to system pressure at constant temperature. The third term was the liquid phase activity and was assumed to be a function of composition and temperature only. The fourth term was the Poynting correction and measured the effect of pressure upon the liquid phase fugacity. The second term was the inverse of the vapor phase component fugacity coefficient which reflected the non-ideality of the vapor-phase mixture of solute and solvent. At low pressure this term was close to unity but became

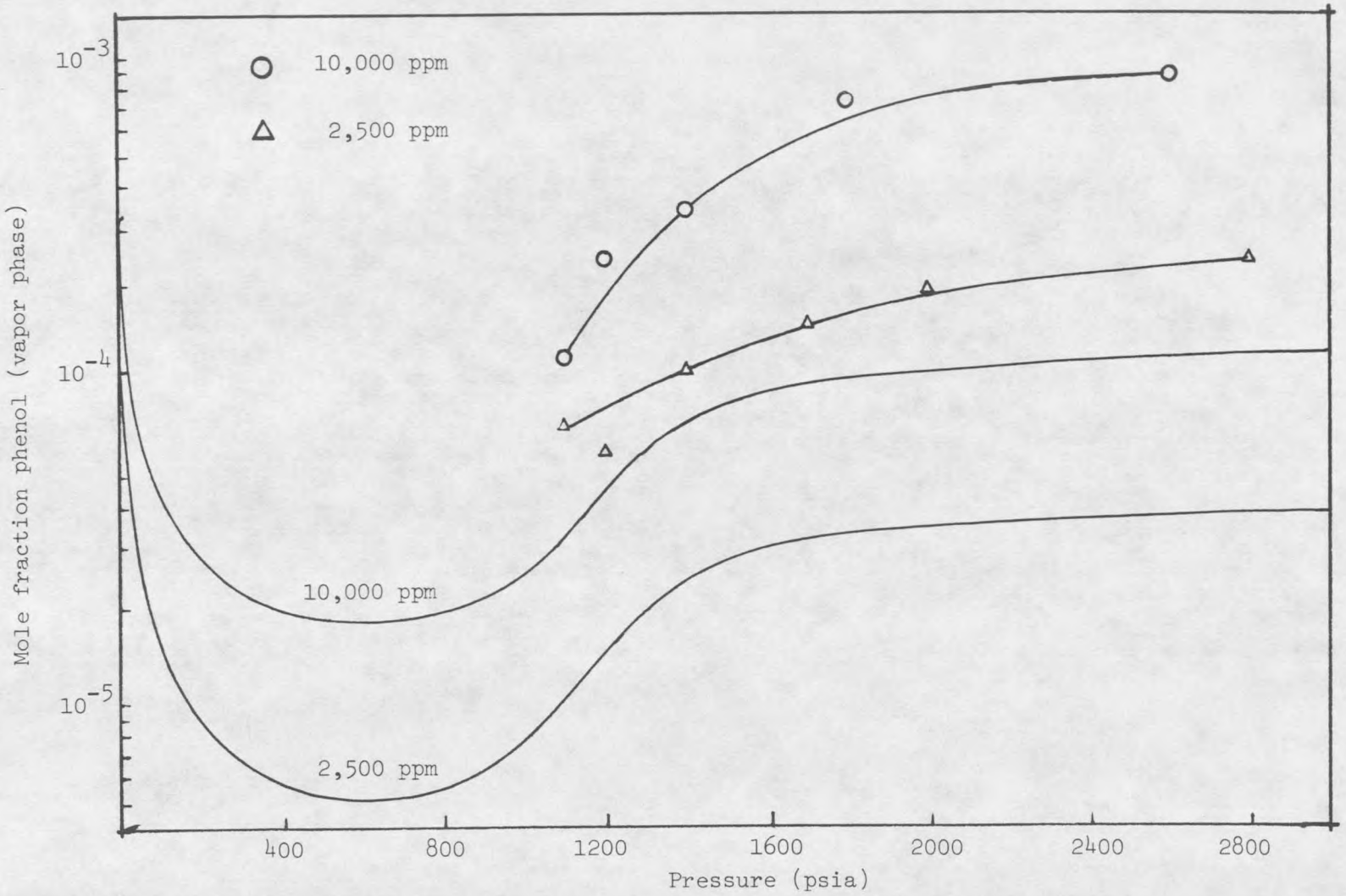


Figure 6. Thermodynamic model-generated vapor phase phenol solubilities and experimental phenol solubilities in supercritical carbon dioxide at 40 degrees Celsius

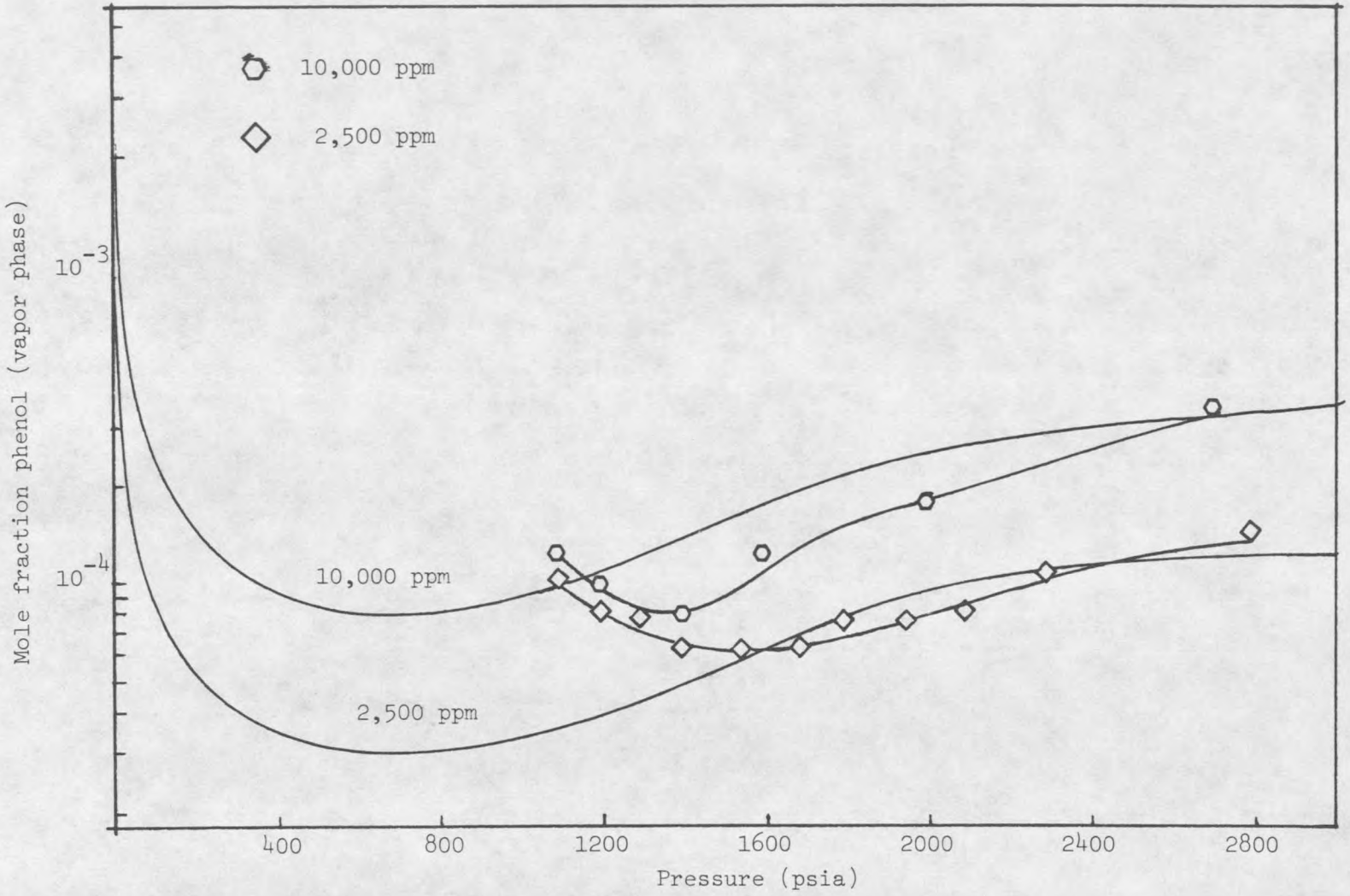


Figure 7. Thermodynamic model-generated vapor phase phenol solubilities and experimental phenol solubilities in supercritical carbon dioxide at 60 degrees Celsius

smaller with higher pressures and thus gave larger vapor phase phenol mole fractions. The model-generated curves showed decreasing vapor phase phenol mole fraction with increasing pressure at low pressures, reflecting the effect of the first term or the ideal solubility. When the pressure reached around 600 psia the vapor phase component fugacity coefficient began to decrease significantly and caused the vapor phase phenol mole fraction to pass through a minimum and continue to increase. Neither the Poynting correction nor the liquid phase activity played an important role in determining the shapes of the vapor phase phenol mole fraction depressions generated by the model.

For both temperatures the model predicted higher vapor phase phenol solubilities for larger phenol solution concentrations. This was a direct result of the mole fraction phenol being larger in the phenol fugacity equation.

Model-generated data differed from the experimental data in Figures 6 and 7 in three respects: (1) the vapor phase phenol solubility was predicted by the model to increase for increasing temperature, (2) the predicted phenol solubilities were four to eight times smaller than the experimental solubilities at 40 degrees Celsius, and (3) the predicted and experimental minimums in phenol solubility occurred at different pressure regions at 60 degrees Celsius. Increased phenol saturation pressures due to increased temperature caused the predicted vapor phase phenol solubilities to increase with increased temperature. The other two discrepancies between experimental and model-generated data might have been caused by the

replacement of unavailable three-component data with two-component data as previously discussed.

Table 3 contains model-generated values of vapor phase composition, vapor phase component fugacity coefficients, and Poynting corrections for phenol and water for their respective pressures at 60 degrees Celsius and 10,000 ppm phenol solution concentration.

Table 3. Aqueous Phenol-Supercritical Carbon Dioxide Model Calculated Values of Mole Fractions in the Vapor Phase, Vapor Phase Component Fugacity Coefficients, and Polnting Corrections for Phenol and Water at 60 degrees Celsius and Phenol Solution Concentration of 10,000 ppm

Press	Vapor Phase Comp. (mole fraction)		Vapor Phase Fugacity Coeff.		Poynting Correction	
(Psia)	Phenol	Water	Phenol	Water	Phenol	Water
10	0.0022	0.290	0.988	0.995	1.00	1.00
50	0.00047	0.059	0.949	0.978	1.01	1.00
100	0.00025	0.030	0.901	0.961	1.02	1.00
200	0.00014	0.016	0.810	0.923	1.05	1.01
400	0.000093	0.0087	0.650	0.848	1.09	1.02
600	0.000082	0.0064	0.514	0.774	1.14	1.03
800	0.000083	0.0053	0.400	0.702	1.20	1.04
1000	0.000091	0.0048	0.305	0.630	1.25	1.05
1100	0.000096	0.0046	0.264	0.595	1.28	1.05
1200	0.00011	0.0045	0.226	0.559	1.31	1.06
1300	0.00012	0.0045	0.193	0.523	1.34	1.06
1400	0.00013	0.0045	0.163	0.487	1.37	1.07
1600	0.00017	0.0047	0.116	0.416	1.43	1.08
1800	0.00022	0.0049	0.085	0.354	1.50	1.09
2000	0.00028	0.0051	0.068	0.307	1.57	1.10
2200	0.00028	0.0053	0.058	0.272	1.64	1.11
2400	0.00030	0.0055	0.052	0.245	1.71	1.12
2600	0.00032	0.0056	0.047	0.224	1.79	1.13
2800	0.00033	0.0057	0.044	0.206	1.87	1.14
3000	0.00035	0.0057	0.042	0.192	1.96	1.15

Design Considerations

This section of the results and discussion presents the experimental vapor-liquid equilibrium data in a form that could be used in predicting the system's extraction capabilities.

Equilibrium phenol mole fractions in the liquid phase and the supercritical carbon dioxide phase are in Table 4 with system pressure and calculated distribution coefficients or equilibrium K-values at 40 degrees Celsius. Figure 8 contains curves of phenol distribution coefficients versus pressure for three different liquid phase phenol mole fractions at 40 degrees Celsius. Figure 8 shows that the phenol distribution coefficient versus system pressure plots for the three

Table 4. Experimental Mole Fractions of Phenol in Water, Mole Fractions of Phenol in Supercritical Carbon Dioxide, and Equilibrium K-values at 40 degrees Celsius

	Mole Fractions Phenol		
Press (psig)	Liquid Phase x	Supercritical Phase y	K-values y/x
1100	0.0019	0.00011	0.058
1100	0.00096	0.00010	0.089
1100	0.00048	0.000070	0.16
1200	0.0019	0.00024	0.13
1200	0.00096	0.00020	0.20
1200	0.00048	0.000058	0.13
1400	0.0019	0.00033	0.17
1400	0.00096	0.00019	0.23
1400	0.00048	0.00010	0.22
1700	0.00096	0.00030	0.31
1700	0.00048	0.00014	0.31
1800	0.0019	0.00069	0.36
2000	0.00096	0.00048	0.50
2000	0.00048	0.00019	0.42
2600	0.0019	0.00082	0.43
2800	0.00096	0.00051	0.53
2800	0.00048	0.00023	0.51

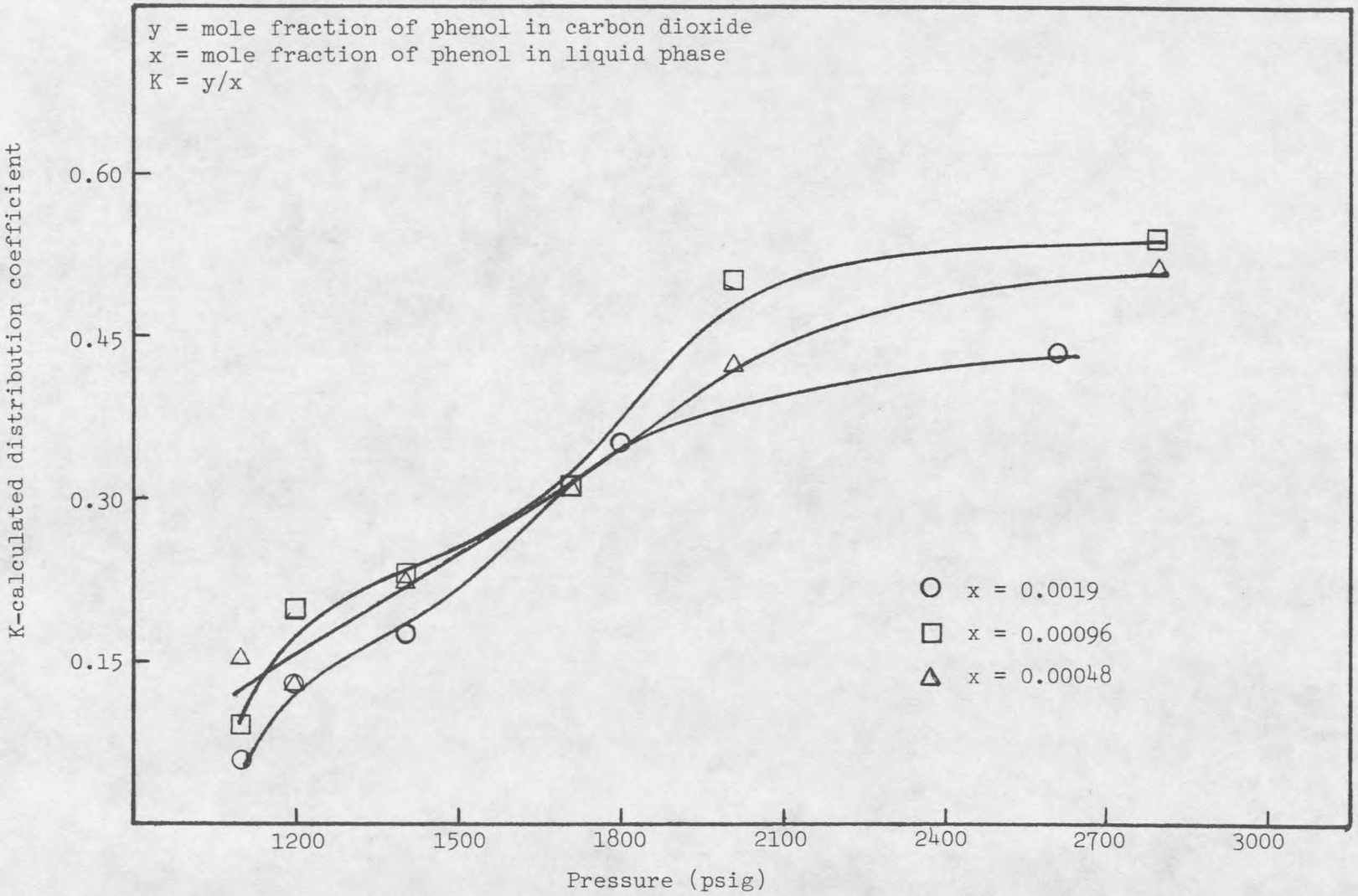


Figure 8. Calculated distribution coefficients of phenol from experimental data for system pressure at 40 degrees Celsius

liquid phase phenol mole fractions were close together at the lower system presures.

Table 5 contains the experimental equilibrium mole fractions of phenol in the liquid phase and supercritical carbon dioxide phase with system pressure and calculated phenol distribution coefficients at 60 degrees Celsius. Figure 9 shows the plots of phenol distribution coefficient versus system pressure for the two different liquid phase phenol mole fractions at 60 degrees Celsius. Figure 9 shows that the distribution coefficient as a function of pressure at constant liquid phase phenol mole fraction passes through a minimum at the lower system pressures for both liquid phase phenol mole fractions.

Table 5. Experimental Mole Fractions of Phenol in Water, Mole Fractions of Phenol in Supercritical Carbon Dioxide, and Equilibrium K-values at 60 degrees Celsius

	Mole Fractions Phenol		
Press (psig)	Liquid Phase x	Supercritical Phase y	K-values y/x
1100	0.0019	0.00012	0.063
1100	0.00048	0.000099	0.22
1200	0.0019	0.000097	0.051
1200	0.00048	0.000080	0.18
1300	0.00048	0.000078	0.17
1400	0.0019	0.000078	0.041
1400	0.00048	0.000061	0.14
1550	0.00048	0.000061	0.14
1600	0.0019	0.00012	0.063
1650	0.00048	0.000062	0.14
1800	0.00048	0.000075	0.17
1950	0.00048	0.000075	0.17
2000	0.0019	0.00017	0.090
2100	0.00048	0.000081	0.18
2300	0.00048	0.00011	0.24
2700	0.0019	0.00034	0.18
2800	0.00048	0.00014	0.31

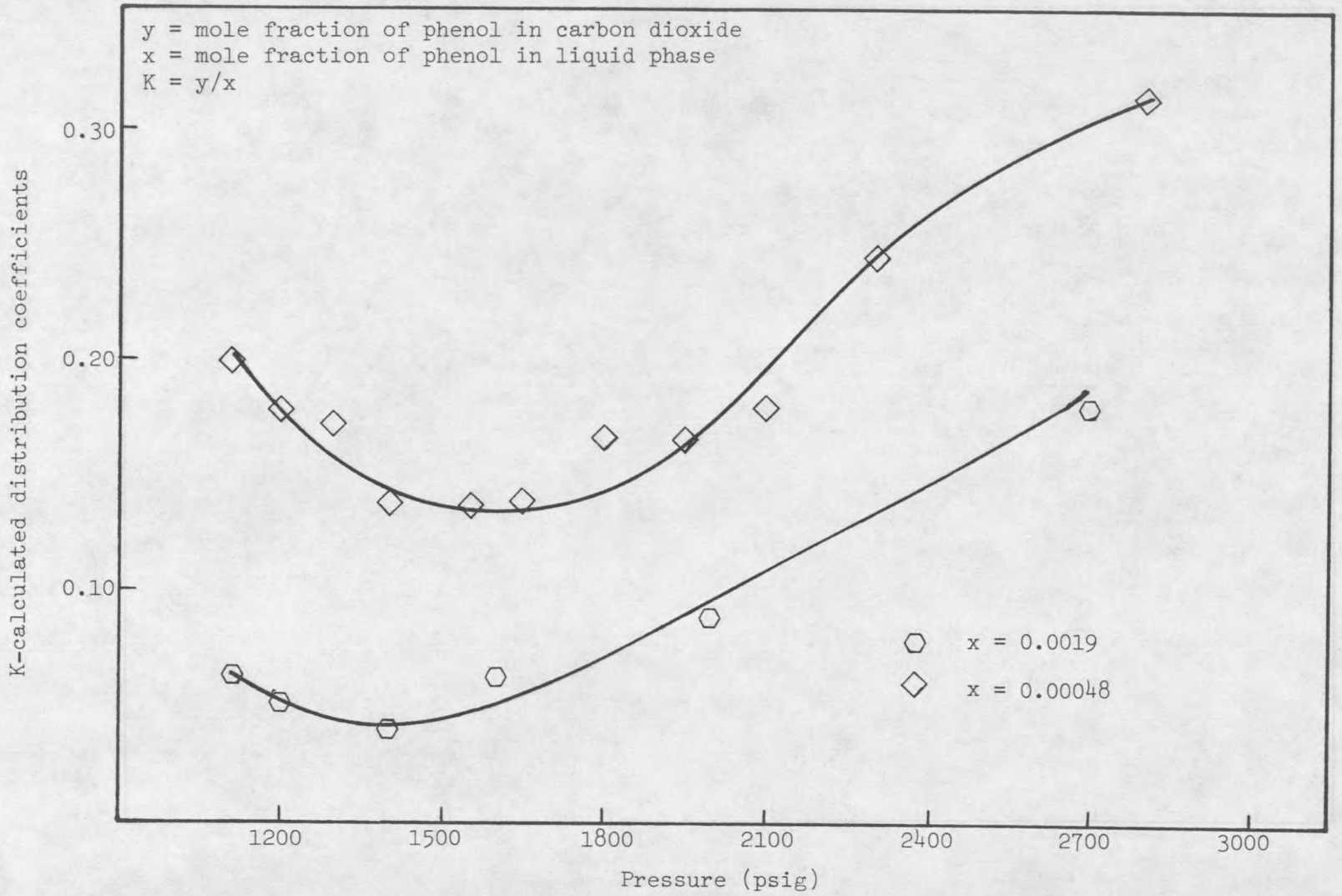


Figure 9. Calculated distribution coefficients of phenol from experimental data for system pressure at 60 degrees Celsius

Gartner investigated the aqueous phenol-supercritical carbon dioxide system at high pressures and measured equilibrium phenol concentrations with a static experimental apparatus [15]. For comparable system pressures and liquid phase phenol concentrations his data yielded larger phenol distribution coefficients (on the order of 10-30% larger). His data is judged to be less reliable because of obvious and large inconsistencies probably due to his cruder experimental methods.

SUMMARY

1. The wet chemistry method of phenol analysis was reproducible with less than 5% error.

2. Pumping liquid carbon dioxide gave stable pressures and satisfactory pressure control.

3. At 40 degrees Celsius the vapor phase phenol solubility increased for increasing pressure.

4. At 60 degrees Celsius there was a minimum in the vapor phase phenol solubility over the studied pressure range for both solution concentrations.

5. Larger phenol solution concentrations gave larger vapor phase phenol solubilities at both temperatures.

6. Lower temperatures gave larger vapor phase phenol solubilities.

7. The data generated by the thermodynamic model of the aqueous phenol-supercritical carbon dioxide system passed through minimums in vapor phase phenol solubilities at both 40 and 60 degrees Celsius in the pressure range of 600 to 700 psia.

8. The model-generated data at 40 degrees Celsius was four to eight times smaller in magnitude than the experimental vapor phase phenol solubility data. At 60 degrees Celsius the model-generated data passed through minimums in vapor phase phenol solubility in different pressure regions than did the experimental vapor phase phenol solubilities. These discrepancies might have been caused by the substitution of unavailable phenol-water-supercritical carbon dioxide three-component

data with phenol-water and water-supercritical carbon dioxide two component data.

9. Calculated distribution coefficients or equilibrium K-values of phenol from the experimental data at 40 degrees Celsius show that phenol K-values increase for increased pressure. At 60 degrees Celsius phenol K-values from experimental data showed minimums in K-values as a function of pressure at lower pressures.

RECOMMENDATIONS FOR FURTHER STUDY

1. Changing the apparatus from a single pass flow system to a vapor recirculation system should be investigated. This would eliminate the handling of the bomb during a run.

2. In-line analysis with high pressure gas chromatography would eliminate the inherent error of manual product collection. It would also drastically reduce the time required for product analysis.

REFERENCES CITED

REFERENCES CITED

1. Bott, T.R., "Supercritical Gas Extraction," Chem. and Indust., March 15, 1980.

2. Van Leer, R.A., and M.E. Paulaitis, "Solubilities of Phenol and Chlorinated Phenols in Supercritical Carbon Dioxide," J. Chem. Eng. Data, 25, 1980.

3. Smith, J.M., and H.C. Van Ness, Introduction to Chemical Engineering Thermodynamics, 3rd ed., McGraw-Hill, New York, 1975.

4. Wilke, G., "Extraction with Supercritical Gases - A Forward," Angew. Chem. Int. Edn., 17, 1978.

5. Peter, S., and G. Brunner, "The Separation of Nonvolatile Substances by Means Compressed Gases in Countercurrent Processes," Angew. Chem. Int. Edn., 17, 1978.

6. Kohn, P.M., and P.R. Savage, "Supercritical Fluids Try For CPI Applications," Chem. Eng., 86(6), 1979.

7. Zosel, K., "Separation with Supercritical Gases: Practical Applications," Angew, Chem, Int. Edn., 17, 1978.

8. Hubert, P., and O.G. Vizthum, "Fluid Extraction of Hops, Spices, and Tobacco with Supercritical Gases," Angew. Chem. Int. Edn., 17, 1978.

9. Modell, M., and R.P. deFilippi, and V.J. Krukonis, "Regeneration of Activated Carbon with Supercritical Carbon Dioxide," presented at the 176th National Meeting of the American Chemical Society, Miami, FL, Sept. 14, 1978.

10. Young, C.L., Chem. Thermo., 2, 1978.

11. Standard Methods for the Examination of Water and Wastewater, American Public Health Association, Washington, DC, 1981.

12. Modell, M., and R.C. Reid, Thermodynamics and Its Applications, 2nd ed., Prentice-Hall, New Jersey, 1983.

13. Hirata, M., and S. One, and K. Nagahama, Computer Aided Data Book of Vapor-Liquid Equilibria, Kodansha Limited Elsevier Scientific Publishing, New York, 1975.

14. Perry, R.H., and C.H. Chilton, Chemical Engineers' Handbook, 5th ed., McGraw-Hill, New York, 1973.

15. Gartner, A.G., "Supercritical Fluid Extraction of Organics From Coal Gasification Wastewaters Using Carbon Dioxide," Master of Science Thesis, Montana State University, 1985.

APPENDICES

APPENDIX A

DERIVATION OF THE THERMODYNAMIC MODEL

DERIVATION OF THE THERMODYNAMIC MODEL

The following vapor and liquid phase component fugacity equations were from Van Ness and Abbott (Van Ness, H.C., and M.M. Abbott, Classical Thermodynamics of Non Electrolyte Solutions, McGraw Hill, New York, 1982, 273). These equations were used to develop the component fugacity equation used to describe phenol and water.

$$\hat{f}_i^L = x_i \gamma_i f_i^0$$

$$\hat{f}_i^V = y_i \hat{\phi}_i P$$

At phase equilibrium

$$\hat{f}_i^L = \hat{f}_i^V$$

Therefore

$$y_i \hat{\phi}_i P = x_i \gamma_i f_i^0$$

The standard state fugacity of pure "i" was chosen to be based upon the standard state associated with the Lewis-Randall rule which was pure "i" at the temperature and pressure of the system.

$$f_i^0 = P_i^{SAT} \times \frac{f_i^{SAT}}{P_i^{SAT}} \times \frac{f_{i(L-R)}}{f_i^{SAT}}$$

Where

$$\frac{f_i^{SAT}}{P_i^{SAT}} = \phi_i^{SAT}$$

For both phenol and water the vapor phase fugacity coefficient of pure "i" at saturation pressure was assumed to be unity. This was due to the moderate saturation pressures of phenol and water at the temperatures investigated. Then the standard state fugacity was represented as:

$$f_i^0 = P_i^{SAT} \times \frac{f_{i(L-R)}}{f_i^{SAT}}$$

Where

$$\ln \frac{f_{i(L-R)}}{f_i^{SAT}} = \int_{P^{SAT}}^{P} \left(\frac{\partial \ln f_i}{\partial P} \right)_T dP$$

$$d \ln f_i = \frac{V_i}{RT} dP$$

Therefore

$$\ln \frac{f_{i(L-R)}}{f_{i_{SAT}}} = \frac{1}{RT} \int_{P^{SAT}}^{P} (V_i)\, dP$$

The term on the right side of the equation is the Poynting correction factor. It was assumed that the specific volume of liquid phenol and water was incompressible and thus, independent of pressure. As a result:

$$\frac{f_{i(L-R)}}{f_i^{SAT}} = \exp\left[\frac{V_i}{RT} (P - P^{SAT})\right]$$

The resultant component fugacity equation which described phenol and water was:

$$y_i \hat{\phi}_i P = x_i \gamma_i P_i^{SAT} \exp\left[\frac{Vi}{RT}(P - P_i^{SAT})\right]$$

For carbon dioxide the vapor phase component fugacity equation was the same equation used for phenol and water. The equation for the liquid phase component fugacity was from Van Ness and Abbott and assumed that the liquid phase activity coefficient based on the standard state associated with Henry's law of carbon dioxide was unity (Van Ness, H.C., and M.M. Abbott, Classical Thermodynamics of Non Electrolyte Solutions, McGraw-Hill, New York, 1982, p. 86).

$$\hat{f}_i^L = x_i H_i$$

$$\hat{f}_i^V = y_i \hat{\phi}_i P$$

The liquid phase was described by Henry's law. Henry's law was chosen due to the low concentrations of carbon dioxide in the liquid phase and available Henry's law constants for carbon dioxide in water. The final equation used to describe carbon dioxide was:

$$y_i \hat{\phi}_i P = x_i H_i$$

Liquid phase mole fractions, x_i, were calculated by setting the number of moles of water and phenol in the liquid solution. Next the amount of the carbon dioxide that would dissolve in the given moles of water was calculated at system conditions using Henry's law constants,

H_i, which were from Perry (Perry, R.H., and C.H. Chilton, Chemical Engineers' Handbook, 5th ed., McGraw-Hill, New York, 1973, p. 3-96).

Liquid phase activity coefficients, γ_i, were calculated from the Wilson equation. Wilson parameters were estimated graphically from phenol-water Wilson parameters at low pressures and temperatures above and below the desired system temperatures (Hirata, M., and S. One, and K. Nagahama, Computer Aided Data Book of Vapor-Liquid Equilibria, Kodansha Limited Elsevier Scientific Publishing, New York, 1975, p. 754-757). The effects of the system's high pressure upon the Wilson parameters were ignored. Also the effects of carbon dioxide in the liquid phase upon the Wilson parameters were ignored.

The saturation pressures, P_i^{SAT}, of water were referenced from steam tables (Smith, J.M., and H.C. Van Ness, Introduction to Chemical Engineering Thermodynamics, 3rd ed., McGraw-Hill, New York, 1975, pp. 572-580). Phenol saturation pressures were from Perry (Perry, R.H., and C.H. Chilton, Chemical Engineers' Handbook, 5th ed., McGraw-Hill, New York, 1973, pp. 3-58).

Specific volumes, V_i, of water were from steam tables (Smith, J.M., and H.C. Van Ness, Introduction to Chemical Engineering Thermodynamics, 3rd ed., McGraw-Hill, New York, 1975, pp. 572-580]. Specific volumes of phenol were from the Handbook of Chemistry and Physics (Weast, R.C., Handbook of Chemistry and Physics 63rd ed., CRC Press, Boca Raton, FL, 1982, p. C-429).

Vapor phase component fugacity coefficients, $\hat{\phi}_i$, were calculated from the Peng-Robinson equation of state. The Peng-Robinson equation of state for vapor phase component fugacity coefficient is given below:

$$\ln\hat{\phi}_i = \ln\frac{\hat{f}_i^v}{y_i P} = \frac{b_i}{b_m}(Z-1) - \ln(Z-B)$$

$$+ \frac{A}{2\sqrt{2}B}\left[\frac{2\sum_k y_k a_{ik}}{a_m} - \frac{b_i}{b_m}\right]\ln\frac{Z+B(1-\sqrt{2})}{Z+B(1+\sqrt{2})}$$

$$A = \frac{amP}{R^2T^2} \qquad B = \frac{bmP}{RT}$$

$$am = \sum_i\sum_j y_i y_j a_{ij} \qquad bm = \sum_i y_i b_i$$

$$a_{ij} = (1-\delta_{ij})(a_i a_j)^{1/2} \qquad a_i \neq a_j$$

$$a_{ii} = a_i$$

$$a_i = \frac{0.4572R^2Tc_i^{\,2}}{Pc_i} \qquad b_i = \frac{0.07780RTc_i}{Pc_i}$$

Values of the binary interaction parameter, δ_{ij}, are usually empirically determined and ordinarily small numbers around 0.10. Therefore all values of δ_{ij} were assumed to be 0.10. Critical properties were from Perry (Perry, R.H., and C.H. Chilton, Chemical Engineers' Handbook, 5th ed., McGraw-Hill, New York, 1973, pp. 3-104, 105). Vapor phase compressibilities, Z, used in the Peng-Robinson equation of state were calculated for pure carbon dioxide at system conditions from the Peng-Robinson equation of state (Modell, M., and R.C. Reid, Thermodynamics and Its Applications, 2nd ed., Prentice-Hall, New Jersey, 1983, pp 152-153). The acentric factor for carbon dioxide

used in calculating compressibilities from the Peng-Robinson equation of state was from Smith and Van Ness (Smith, J.M., and H.C. Van Ness, Introduction to Chemical Engineering Thermodynamics, 3rd ed., McGraw-Hill, New York, 1975, p. 570).

APPENDIX B

COMPUTER AIDED SOLUTIONS OF THE THERMODYNAMIC MODEL OF AQUEOUS PHENOL-SUPERCRITICAL CARBON DIOXIDE VAPOR-LIQUID EQUILIBRIUM

COMPUTER AIDED SOLUTIONS OF THE THERMODYNAMIC MODEL

Figures 10 and 11 show two computer solution methods for 40 degrees Celsius and 10,000 ppm and 60 degrees Celsius and 10,000 ppm respectively. These methods of solution include the method that used all three of the component fugacity equations (method 1), and the method that used two of the component fugacity equations and a vapor phase mole balance (method 2).

The computer program used to calculate the data for the second method at 60 degrees and 10,000 ppm phenol solution concentration follows the above mentioned figures.

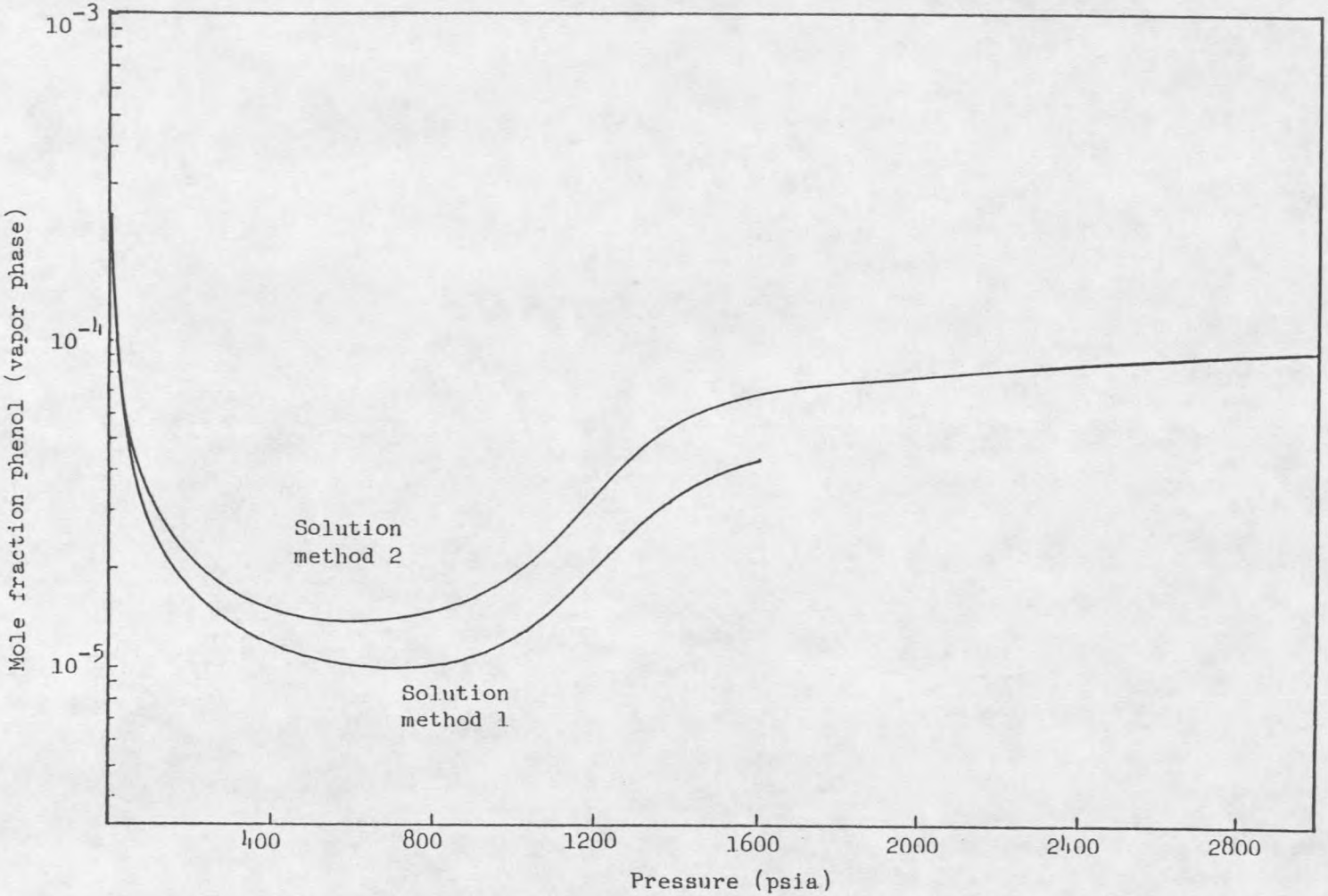


Figure 10. Comparison of two solution methods of the aqueous phenol-supercritical carbon dioxide thermodynamic model at 40 degrees Celsius (method 1 used all three of the component fugacity equations and method 2 used two of the component fugacity equations and a vapor phase mole balance)

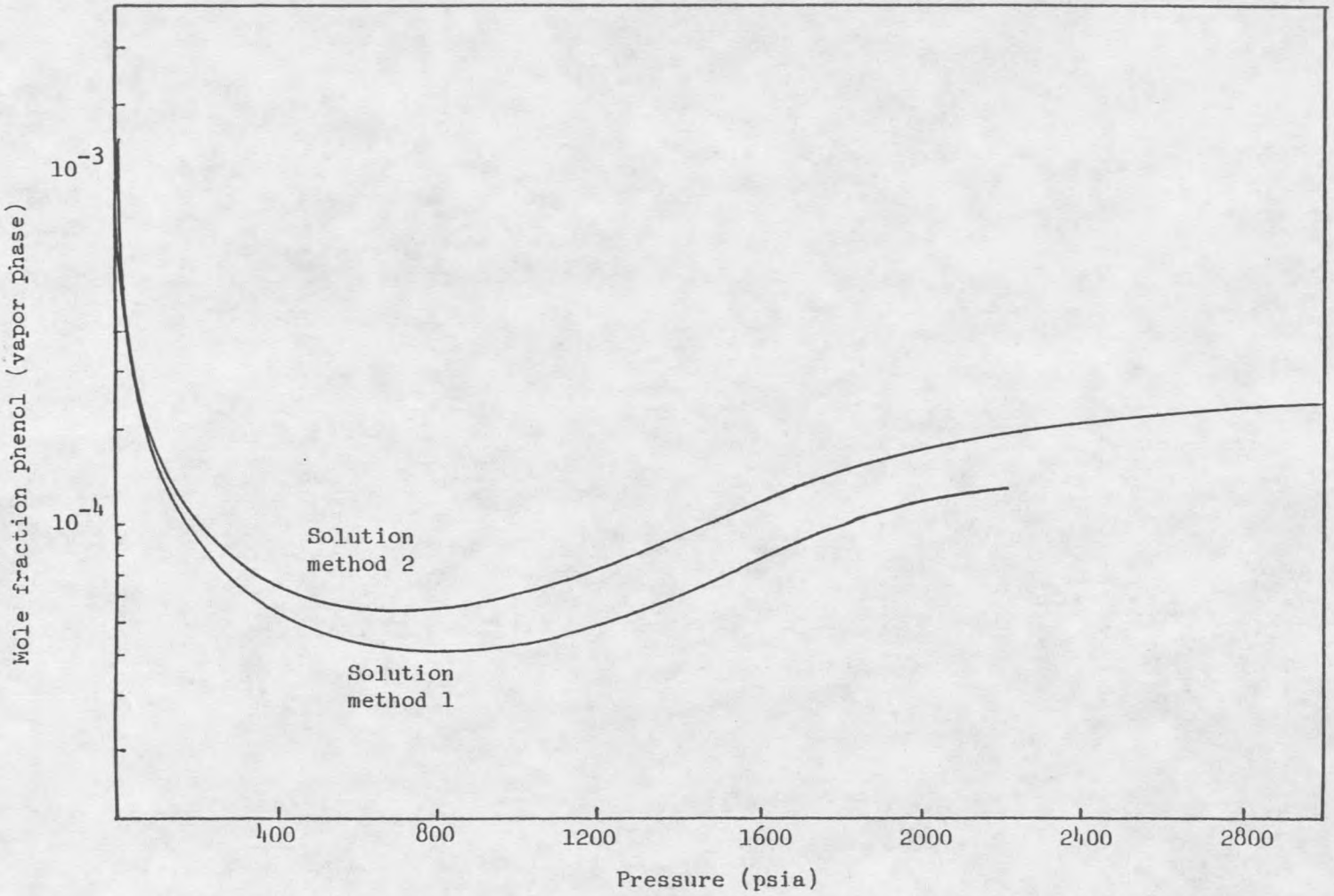


Figure 11. Comparison of two solution methods of the aqueous phenol-supercritical carbon dioxide thermodynamic model at 60 degrees Celsius (method 1 used all three of the component fugacity equations and method 2 used two of the component fugacity equations and a vapor phase mole balance)

```
CCCCCCCCCCCCCCCCCCCCCCCCCCCCCCCCCCCCCCCCCCCCCCCCCCCCCCCCCCCCCCCCCCCCCCCCCCCCCCC
C                                                                              C
C     LISTING OF CONSTANTS INDEPENDANT OF P & T                                C
C                                                                              C
C     PHENOL=1  WATER=2  SUPERCRITCAL CO2=3                                    C
C                                                                              C
CCCCCCCCCCCCCCCCCCCCCCCCCCCCCCCCCCCCCCCCCCCCCCCCCCCCCCCCCCCCCCCCCCCCCCCCCCCCCCC
C
C     CRITICAL PROPERTIES
C
      REAL HL3,MCO2,K
      TC1=694.2
      TC2=647.3
      TC3=304.2
      PC1=60.5
      PC2=217.6
      PC3=72.8
C
C     BINARY INTERACTION PARAMETERS
C
      WRITE(6,30)
      READ(5,*)DEL1,DEL2
      R=82.051
C
C     PENG-ROBINSON EQUATION CONSTANTS
C
      K=.707984
      A1=.45724*(R*TC1)**2./PC1
      A2=.45724*(R*TC2)**2./PC2
      A3=.45724*(R*TC3)**2./PC3
      B1=.0778*R*TC1/PC1
      B2=.0778*R*TC2/PC2
      B3=.0778*R*TC3/PC3
      A4=(1.-DEL2)*((A1*A2)**.5)
      A5=(1.-DEL1)*((A1*A3)**.5)
      A6=(1.-DEL1)*((A2*A3)**.5)
CCCCCCCCCCCCCCCCCCCCCCCCCCCCCCCCCCCCCCCCCCCCCCCCCCCCCCCCCCCCCCCCCCCCCCCCCCCCCCC
C                                                                              C
C     DATA INPUT                                                               C
C                                                                              C
CCCCCCCCCCCCCCCCCCCCCCCCCCCCCCCCCCCCCCCCCCCCCCCCCCCCCCCCCCCCCCCCCCCCCCCCCCCCCCC
 4    WRITE(6,35)
      READ(5,*)T,P
      WRITE(6,40)
      READ(5,*)Y1,Y2
      WRITE(6,45)
      READ(5,*)TOL
```

Figure 12. Computer program to calculate the vapor-liquid equilibrium of the aqueous phenol-supercritical carbon dioxide system

Figure 12. continued

```
CCCCCCCCCCCCCCCCCCCCCCCCCCCCCCCCCCCCCCCCCCCCCCCCCCCCCCCCCCCCCCCCCCCCCCCCCCCCCCC
C                                                                              C
C     TEMP DEPENDANT PRESS INDEPENDANT CONSTANTS                               C
C                                                                              C
CCCCCCCCCCCCCCCCCCCCCCCCCCCCCCCCCCCCCCCCCCCCCCCCCCCCCCCCCCCCCCCCCCCCCCCCCCCCCCC
C
C     40 C CONSTANTS
C
      IF(T.EQ.333.) GO TO 1
      P1SAT=.00146
      P2SAT=.07279
      SPVOL1=90.
      SPVOL2=18.14
      WP12=.0080
      WP21=.820
      GO TO 2
C
C     60 C CONSTANTS
C
 1    P1SAT=.00566
      P2SAT=.19660
      SPVOL1=90.
      SPVOL2= 18.31
      WP12=.0052
      WP21=.744
CCCCCCCCCCCCCCCCCCCCCCCCCCCCCCCCCCCCCCCCCCCCCCCCCCCCCCCCCCCCCCCCCCCCCCCCCCCCCCC
C                                                                              C
C     PRESS DEPENDANT CONSTANTS                                                C
C                                                                              C
CCCCCCCCCCCCCCCCCCCCCCCCCCCCCCCCCCCCCCCCCCCCCCCCCCCCCCCCCCCCCCCCCCCCCCCCCCCCCCC
C
C     LIQUID SOLUTION COMPOSITIONS
C
C     40 C
C
 2    P=P/14.7
      IF(T.EQ.333.) GO TO 3
      HL3=EXP(7.8013+(.2306E-2)*P+(.5801E-4)*P**2.-(.1999E-6)*P**3.)
      X3=P/HL3
      MCO2=X3*55.666/(1.-X3)
      TMOL=55.666+MCO2
      X1=.1063/TMOL
      X2=55.56/TMOL
      WRITE(6,*)X1,X2
C
C     ACTIVITY COEFFCIENTS FROM THE WILSON EQUATION
C
      WEQC=WP12/(X1+X2*WP12)-WP21/(X2+X1*WP21)
      ACOEF1=EXP(LOG(1./(X1+X2*WP12))+X2*WEQC)
      ACOEF2=EXP(LOG(1./(X2+X1*WP21))-X1*WEQC)
      GO TO 14
C
C     60 C
C
 3    HL3=EXP(8.144+(.3204E-2)*P+(.2051E-4)*P**2.-(.6298E-7)*P**3.)
      X3=P/HL3
```

Figure 12. continued

```
      MCO2=X3*55.666/(1.-X3)
      TMOL=55.666+MCO2
      X1=.1063/TMOL
      X2=55.56/TMOL
      WRITE(6,*)X1,X2
C
C     ACTIVITY COEFFCIENTS FROM THE WILSON EQUATION
C
      WEQC=WP12/(X1+X2*WP12)-WP21/(X2+X1*WP21)
      ACOEF1=EXP(LOG(1./(X1+X2*WP12))+X2*WEQC)
      ACOEF2=EXP(LOG(1./(X2+X1*WP21))-X1*WEQC)
C
C     VAPOR PHASE COMPRESSIBILITIES FROM THE PENG-ROBINSON
C     EQUATION OF STATE
C
 14   ALPHA=(1.+K*(1.-((T/TC3)**.5)))**2.
      V=90.
 5    VOL=R*T/(P+A3*ALPHA/(V*(V+B3)+B3*(V-B3)))+B3
      CALL CONV(V,VOL,1,NC)
      GO TO (6,5),NC
 6    Z=P*VOL/(R*T)
C
C
C     VAPOR PHASE COMPOSITION CONVERGENCE LOOPS
C
C     FIRST LOOP
C
 9    Y3=1.-(Y1+Y2)
      PC1=EXP(SPVOL1*(P-P1SAT)/(R*T))
 7    Y1C=X1*ACOEF1*P1SAT*PC1/P/(EXP(B1*(Z-1.)/(Y1*B1+Y2*B2+Y3*B3)-
     @LOG(Z-P*(Y1*B1+Y2*B2+Y3*B3)/(R*T))+(Y1**2.*A1+Y2**2.*A2+
     @Y3**2.*A3+2.*Y1*Y2*(1.-DEL2)*(A1*A2)**.5+2.*Y1*Y3*(1.-DEL1)*(A1*
     @A3)**.5+2.*Y2*Y3*(1.-DEL1)*(A2*A3)**.5)/(2.8284*(Y1*B1+Y2*B2+Y3*
     @B3)*(R*T))*((Y1*A1+Y2*A4+Y3*A5)*2./(Y1**2.*A1+Y2**2.*A2+Y3**2.*A3
     @+2.*Y1*Y2*(1.-DEL2)*(A1*A2)**.5+2.*Y1*Y3*(1.-DEL1)*(A1*A3)**.5
     @+2.*Y2*Y3*(1.-DEL1)*(A2*A3)**.5)-B1/(Y1*B1+Y2*B2+Y3*B3))*LOG(
     @(Z-.4142*P/(R*T)*(Y1*B1+Y2*B2+Y3*B3))/(Z+2.4142*P/(R*T)*(Y1*B1
     @+Y2*B2+Y3*B3)))))
      CALL CONV(Y1,Y1C,1,NC)
      GO TO (8,7),NC
C
C     CHECK FOR Y2CALC-Y2 CONVERGENCE
C
 8    AM=Y1**2.*A1+Y2**2.*A2+Y3**2.*A3+2.*Y1*Y2*(1.-DEL2)*(A1*A2)**.5
     @+2.*Y1*Y3*(1.-DEL1)*(A1*A3)**.5+2.*Y2*Y3*(1.-DEL1)*(A2*A3)**.5
      BM=Y1*B1+Y2*B2+Y3*B3
      A=AM*P/((R*T)**2.)
      B=BM*P/(R*T)
      PHI2=EXP(B2*(Z-1.)/BM-LOG(Z-B)+A/(2.8284*B)*((Y1*A4+Y2*A2+Y3*A6
     @)*2./AM-B2/BM)*LOG((Z-B*.4142)/(Z+B*2.4142)))
      PC2=EXP(SPVOL2*(P-P2SAT)/(R*T))
      Y2C=X2*ACOEF2*P2SAT/(PHI2*P)*PC2
      WRITE(6,*)Y1,Y2,Y2C,Y3
      S=2.*ABS(Y2C-Y2)/(Y2C+Y2)
      IF(S.LE.TOL) GO TO 11
C
C     SECOND LOOP
```

Figure 12. continued

```
C
      PC2=EXP(SPVOL2*(P-P2SAT)/(R*T))
 10   Y2C=X2*ACOEF2*P2SAT*PC2/P/(EXP(B2*(Z-1.)/(Y1*B1+Y2*B2+Y3*B3)-
     @LOG(Z-P/(R*T)*(Y1*B1+Y2*B2+Y3*B3))+(Y1**2.*A1+Y2**2.*A2+Y3**2.
     @*A3+2.*Y1*Y2*(1.-DEL2)*(A1*A2)**.5+2.*Y1*Y3*(1.-DEL1)*(A1*A3)**.5
     @+2.*Y2*Y3*(1.-DEL1)*(A2*A3)**.5)/(2.8284*R*T)/(Y1*B1+Y2*B2+Y3*B3)
     @*((Y1*A4+Y2*A2+Y3*A6)*2./(Y1**2.*A1+Y2**2.*A2+Y3**2.*A3+2.*Y1*Y2
     @*(1.-DEL2)*(A1*A2)**.5+2.*Y1*Y3*(1.-DEL1)*(A1*A3)**.5+2.*Y2*Y3*(1.
     @-DEL1)*(A2*A3)**.5)-B2/(Y1*B1+Y2*B2+Y3*B3))*LOG((Z-.4142*P/(R*T)*
     @(Y1*B1+Y2*B2+Y3*B3))/(Z+2.4142*P/(R*T)*(Y1*B1+Y2*B2+Y3*B3)))))
      CALL CONV(Y2,Y2C,1,NC)
      WRITE(6,*)Y1,Y2,Y2C,Y3
      GO TO (9,10),NC
C
C     CHECK FOR Y3CALC-Y3 CONVERGENCE
C
 11   Y3C=1.-(Y1+Y2)
      WRITE(6,*)Y1,Y2,Y3C,Y3
      S1=2.*ABS(Y3C-Y3)/(Y3C+Y3)
      IF(S1.LE.TOL) GO TO 12
      GO TO 9
C
C     PRINT OUT SOLUTION TO VAPOR PHASE COMPOSITION FOR
C     GIVEN PRESSURE AT SYSTEM TEMPERATURE
 12   PHI1=X1*ACOEF1*P1SAT*PC1/P/Y1
      PHI2=X2*ACOEF2*P2SAT*PC2/P/Y2
      WRITE(6,*)T,P,Y1,Y2,Y3
      WRITE(6,*)PHI1,PHI2
      WRITE(1,50)T,P*14.7
      WRITE(1,55)
      WRITE(1,60)Y1,Y2,Y3
      WRITE(1,65)
      WRITE(1,70)PHI1,PHI2,PC1,PC2
C
C     INCREMENT PRESSURE OR ASK FOR NEW PRESSURE OR END
C
      WRITE(6,75)
      READ(5,*)P
      IF(P.EQ.1.) GO TO 13
      IF(P.EQ.10.) GO TO 4
      GO TO 2
C
C     FORMAT STATEMENTS FOR OUTPUT
C
 30   FORMAT(3X,'INPUT BIN INTRCTN PARAMTR; VAP-LIQ, LIQ-LIQ')
 35   FORMAT(3X,'ENTER TEMP ( DEG K ) , ENTER BEG PRESSURE ( PSIA )')
 40   FORMAT(3X,'ENTER INITIAL GUESS FOR; Yphenol, Ywater')
 45   FORMAT(3X,'ENTER CONVERGENCE CRITERION')
 50   FORMAT(///1X,'TEMP=',F6.2,1X,'K ',5X,'PRESS=',F6.1,1X,'PSIA')
 55   FORMAT(/10X,'  VAPOR PHASE COMPOSITION ( MOLE FRACTION )'//
     @15X,'PHENOL',10X,'WATER',10X,'CO2')
 60   FORMAT(/15X,F8.7,8X,F8.7,7X,F8.7)
 65   FORMAT(//10X,'VAPOR PHASE FUGACITY COEFFS',5X,'POYNTING
     @ CORRECTION',//10X,'PHENOL',10X,'WATER',11X,'PHENOL',9X,'WATER')
 70   FORMAT(/10X,F9.8,7X,F9.8,6X,F5.2,10X,F5.2)
 75   FORMAT(1X,'ENTER NEW PRESS (PSIA); ENTER 10 FOR NEW TEMP, ENTER
     @ 1 FOR PROGRAM END')
 13   END
```

APPENDIX C

SPECTROPHOTOMETRIC PHENOL ANALYSIS

CALIBRATION CURVE OF ABSORBANCE

VERSUS PHENOL CONCENTRATION

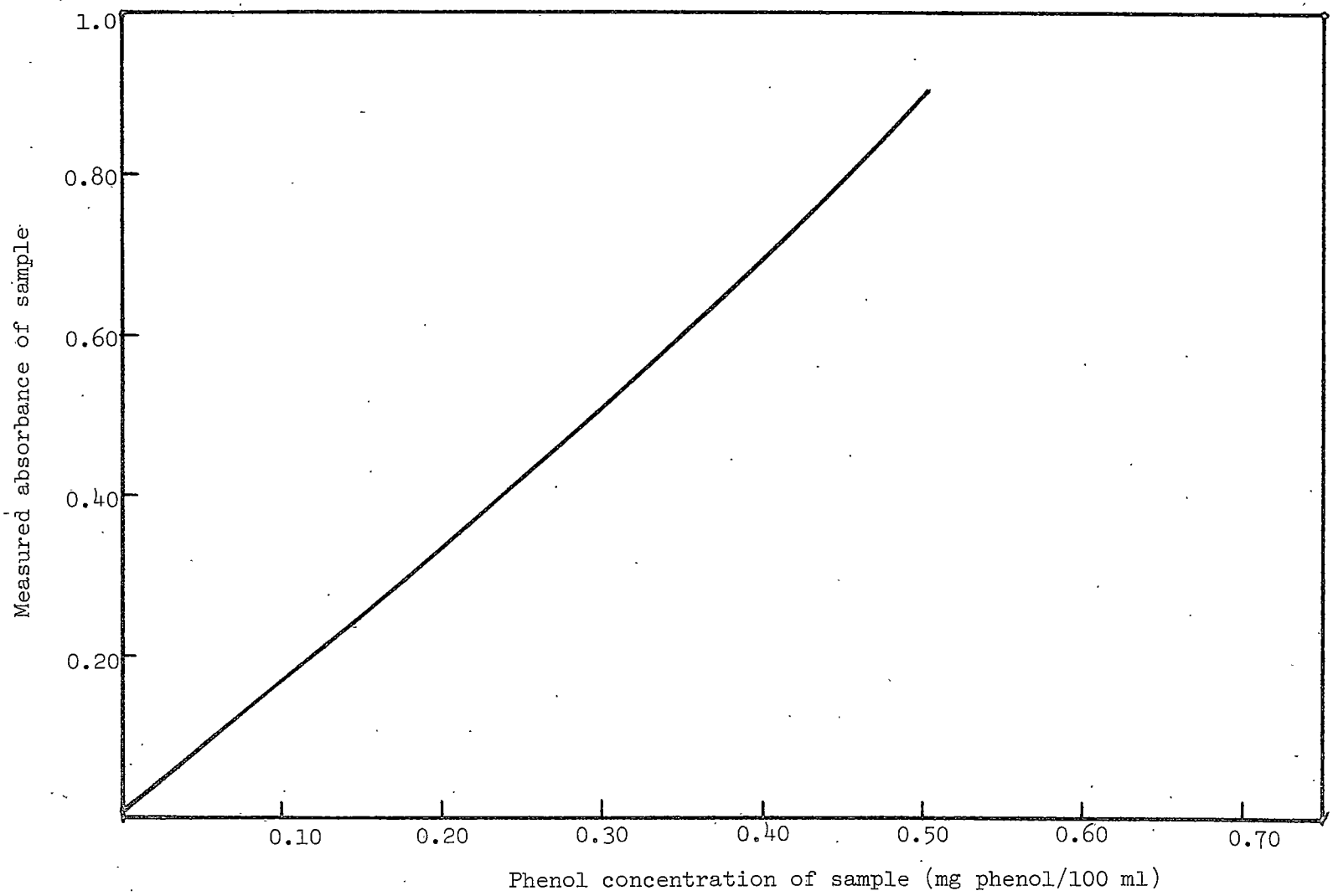


Figure 13. Phenol analysis calibration curve of absorbance versus phenol concentration.



Main
N378
L538
cop.2